Applied Energy 276 (2020) 115522

Contents lists available at ScienceDirect

Applied Energy

journal homepage: www.elsevier.com/locate/apenergy

Modelling of national and local interactions between heat and electricity networks in low-carbon energy systems

Marko Aunedi[a,*], Antonio Marco Pantaleo[b,c], Kamal Kuriyan[b], Goran Strbac[a], Nilay Shah[b]

[a] Department of Electrical and Electronic Engineering, Imperial College London, UK
[b] Department of Chemical Engineering, Imperial College London, UK
[c] Department of Agro-Environmental Sciences, University of Bari Aldo Moro, Italy

HIGHLIGHTS

- Paper presents a novel approach for optimising the mix of heat supply technologies.
- Heat supply choices are affected by local and national interactions with power.
- Heat sector flexibility can support decarbonisation of electricity supply.
- Emission limits and grid constraints shape the optimal heat plant portfolio.
- Increasing heat storage capacity can help with local network constraints.

ARTICLE INFO

Keywords:
District heating
Polygeneration
Combined heat and power
Heat pumps
Thermal energy storage
System integration

ABSTRACT

Decarbonisation of the heating and cooling sector is critical for achieving long-term energy and climate change objectives. Closer integration between heating/cooling and electricity systems can provide additional flexibility required to support the integration of variable renewables and other low-carbon energy sources. This paper proposes a framework for identifying cost-efficient solutions for supplying district heating systems within both operation and investment timescales, while considering local and national-level interactions between heat and electricity infrastructures. The proposed optimisation model minimises the levelised cost of a portfolio of heating technologies, and in particular Combined Heat and Power (CHP) and polygeneration systems, centralised heat pumps (HPs), centralised boilers and thermal energy storage (TES). A number of illustrative case studies are presented, quantifying the impact of renewable penetration, electricity price volatility, local grid constraints and local emission targets on optimal planning and operation of heat production assets. The sensitivity analysis demonstrates that the cost-optimal TES capacity could increase by 41–134% in order to manage a constraint in the local electricity grid, while in systems with higher RES penetration reflected in higher electricity price volatility it may be optimal to increase the TES capacity by 50–66% compared to constant prices, allowing centralised electric HP technologies to divert excess electricity produced by intermittent renewable generators to the heating sector. This confirms the importance of reflecting the whole-system value of heating technologies in the underlying cost-benefit analysis of heat networks.

1. Introduction

Together with reducing the carbon impact of the electricity sector through the deployment of low-carbon technologies such as renewables or nuclear generation, decarbonisation of the heating and cooling sector will be critical for achieving EU's long-term energy and climate change objectives. Heating and cooling currently account for half of the EU's energy consumption and for a similar proportion of the total carbon emissions [1], with three quarters of energy still being provided by fossil fuels (mostly natural gas). It has been shown that heating and electricity systems can benefit significantly from mutual synergies on their pathways towards decarbonisation [2], by unlocking opportunities for cross-vector flexibility to support the integration of low-carbon generation technologies and to significantly reduce the cost of decarbonisation [3]. Integrated planning and operation of district heating, gas, hydrogen and electricity networks offers interesting

* Corresponding author.
E-mail addresses: m.aunedi@imperial.ac.uk (M. Aunedi), a.pantaleo@imperial.ac.uk (A.M. Pantaleo), k.kuriyan@imperial.ac.uk (K. Kuriyan), g.strbac@imperial.ac.uk (G. Strbac), n.shah@imperial.ac.uk (N. Shah).

https://doi.org/10.1016/j.apenergy.2020.115522
Received 31 January 2020; Received in revised form 17 June 2020; Accepted 14 July 2020

Nomenclature

Indices

t	Time interval
d	Characteristic day
i	CHP plant unit
j	Large-scale HP unit
k	Heat storage unit
l	Boiler unit

Parameters

T	Number of time intervals in a characteristic day (typically 24 or 48)
Δ	Duration of the unit interval (in hours)
D	Number of characteristic days used in the study
N_d	Frequency (number of occurrences) of characteristic day d within a year
I	Number of CHP units
J	Number of large-scale HP units
K	Number of heat storage units
L	Number of boiler units
C_{VOLL}	Value of Lost Load (VOLL), cost associated with unserved heat demand (in €/MW_{th})
$H_{t,d}$	Heat demand profile at time t for day d (including losses) (in MW_{th})
$D_{t,d}^{el}$	Baseline electricity demand profile at local substation at time t for day d (in MW_{el})
$B_{E,t,d}$	Electricity price profile at time t for day d (in €/MWh_{el})
E_{CO_2}	Annual limit on CO_2 emissions from the heat supply system (in tonnes of CO_2)
E_{NO_x}	Annual limit on NO_x emissions from the heat supply system (in tonnes of NO_x)
E_{PM}	Annual limit on particulate matter (PM) emissions from the heat supply system (in tonnes of PM)
$E_t^{gridCO_2}$	Carbon intensity of electricity grid at time t (in tCO_2/MWh_{el})
G_{cap}	Capacity of local electricity grid (substation) (in MW_{el})
α	Factor for constraining reverse power flows at substation
$P_{CHP,i}^{MAX}$	Maximum installed capacity of CHP unit i (in MW_{el})
$\Gamma_{CHP,i}^{min}$	Minimum electricity output relative to installed capacity for CHP unit i
$P_{HP,j}^{MAX}$	Maximum installed capacity of large HP unit j (in MW_{el})
$H_{S,k}^{MAX}$	Maximum installed capacity of heat storage unit k (in MW_{th})
$H_{B,l}^{MAX}$	Maximum installed capacity of boiler unit l (in MW_{th})
$I_{CHP,i}^{F}$	Fixed component of (annualised) investment cost for CHP unit i (in €/yr)
$I_{HP,j}^{F}$	Fixed component of (annualised) investment cost for large HP unit j (in €/yr)
$I_{S,k}^{F}$	Fixed component of (annualised) investment cost for heat storage unit k (in €/yr)
$I_{B,l}^{F}$	Fixed component of (annualised) investment cost for boiler unit l (in €/yr)
$I_{CHP,i}^{V}$	Variable component of (annualised) investment cost for CHP unit i (in €/kW_{el}/yr)
$I_{HP,j}^{V}$	Variable component of (annualised) investment cost for large HP unit j (in €/kW_{el}/yr)
$I_{S,k}^{V}$	Variable component of (annualised) investment cost for heat storage unit k (in €/kW_{th}/yr)
$I_{B,l}^{V}$	Variable component of (annualised) investment cost for boiler unit l (in €/kW_{th}/yr)
$A_{CHP,i}$	Unit no-load generation cost of CHP unit i (in €/MWh_{el})
$B_{CHP,i}$	Variable electricity generation cost of CHP unit i (in €/MWh_{el})
$F_{B,l}$	Fuel cost of boiler unit l (in €/MWh)
$R_{CHP,i}$	Ratio between heat and electricity output for CHP unit i
$R_{HP,j}$	Ratio between heat output and electricity input (COP) for large HP unit j
$D_{S,k}$	Duration (ratio between energy and power rating) for heat storage unit k (in hours)
$\eta_{S,k}$	Roundtrip efficiency of heat storage unit k
$W_{S,k}^{min}$	Minimum relative SoC of heat storage unit k
$\eta_{B,l}$	Combustion efficiency of boiler unit l
$E_{CHP,i}^{CO_2}$	Emission factor for CO_2 per unit of electricity output of CHP unit i (in tCO_2/MWh_{el})
$E_{CHP,i}^{NO_x}$	Emission factor for NO_x per unit of electricity output of CHP unit i (in tonnes of NO_x per MWh_{el})
$E_{CHP,i}^{PM}$	Emission factor for PM per unit of electricity output of CHP unit i (in tonnes of PM per MWh_{el})
$E_{B,l}^{CO_2}$	Emission factor for CO_2 per unit of heat output of boiler unit l (in tCO_2/MWh_{th})
$E_{B,l}^{NO_x}$	Emission factor for NO_x per unit of heat output of boiler unit l (in tonnes of NO_x per MWh_{th})
$E_{B,l}^{PM}$	Emission factor for PM per unit of heat output of boiler unit l (in tonnes of PM per MWh_{th})

Decision variables

$c_{CHP,i}$	Investment cost into CHP unit i (in €/yr)
$c_{HP,j}$	Investment cost into large-scale HP unit j (in €/yr)
$c_{S,k}$	Investment cost into heat storage unit k (in €/yr)
$c_{B,l}$	Investment cost into boiler unit l (in €/yr)
$u_{CHP,i}$	Binary decision on investment into CHP unit i
$u_{HP,j}$	Binary decision on investment into large HP unit j
$u_{S,k}$	Binary decision on investment into heat storage unit k
$u_{B,l}$	Binary decision on investment into boiler unit l
$\pi_{CHP,i}$	Installed capacity of CHP unit i
$\pi_{HP,j}$	Installed capacity of large HP unit j
$\pi_{S,k}$	Installed capacity of heat storage unit k
$\pi_{B,l}$	Installed capacity of boiler unit l
$\delta_{CHP,i,t,d}$	Binary decision on whether the CHP unit i is turned on at time t for day d
$p_{CHP,i,t,d}$	Electrical output of CHP unit i at time t for day d (in MW_{el})
$\omega_{CHP,i,t,d}$	Operating cost of CHP unit i at time t for day d (in €)
$p_{HP,j,t,d}$	Electrical input of large HP unit j at time t for day d (in MW_{el})
$h_{CHP,i,t,d}$	Heat output of CHP unit i at time t for day d (in MW_{th})
$h_{HP,i,t,d}$	Heat output of large HP unit j at time t for day d (in MW_{th})
$h_{S,k,t,d}^{+}$	Heat output (discharging) from heat storage unit k at time t for day d (in MW_{th})
$h_{S,k,t,d}^{-}$	Heat input (charging) into heat storage unit k at time t for day d (in MW_{th})
$h_{B,l,t,d}$	Heat output of boiler unit l at time t for day d (in MW_{th})
$w_{S,k,t,d}$	State of charge of heat storage unit k at time t for day d (in MWh_{th})
$h_{curt,t,d}$	Curtailed heat demand at time t for day d (in MW_{th})

opportunities for a broad range of technologies, including flexible co-generation systems, power to gas or demand side management options [4,5]. Energy storage plays a critical role in balancing the operation of integrated networks with variable supply and demand. It has been shown that seasonal storage is especially useful when a significant reduction in emissions is required, when a large amount of intermittent renewable generation is available, or when the system is characterised by a large ratio of thermal to electrical demand [6].

1.1. Interactions in multi-carrier energy networks

The effectiveness of linkages between gas, power, heating, and water resources and their interdependency in optimal operation and design of multi-carrier energy networks is a research topic that has gained broad interest in recent literature. A security-constrained framework for interconnected power and gas systems was proposed in [7], while the optimal operation of integrated energy systems while taking into account the uncertainty of wind generation was proposed in [8], introducing an incentive-based demand-response strategy to modulate both gas and electricity loads. A number of a bi-level frameworks have been introduced for optimal energy management of integrated gas and electricity networks, minimizing the combined network operation cost and maximizing the private owners' profits [9,10], exploring the expansion planning and optimal integrated operation of these networks [11], or including minimisation of operation cost and emissions of pollutant gases [12].

Recent work in this area has also focused on modelling electricity to heating technologies and the impact of electricity prices on heat supply and the profitability of district heating networks [13], as well as on the impact of fluctuating energy prices on operation strategies of polygeneration systems coupled with energy networks [14]. Energy technologies linking heat and power will play a key role in the integration between heating/cooling and electricity networks, and therefore a lot of research has focused on the optimal design and operation of embedded polygeneration systems and their integration with energy networks, including natural gas and biomass dual source technologies [15,16], hybrid solar-biomass systems [17,18], gas/renewable energy source integrated polygeneration systems [19], different typologies of building-integrated vs. centralised heat pumps [20,21,22], or thermal energy storage options for district heating [23]. A model for cost-optimal long-term multi-area combined heat and power production with heat and power storage and power transmission between areas has been presented in [24], minimizing the total production and transmission cost using a novel decomposition method to solve larger systems.

1.2. Planning and operation of DHN

A number of recent studies have shown that district heating (DH) can play an important role in the evolution towards sustainable energy systems [25,26,27], but also that the present district heating networks (DHN) must undergo a radical change to become an integral part of smart energy systems. Various approaches to heat supply planning have been proposed in the literature [28,29]. Another common optimisation problem in this area is district heating network design, for which methods have been proposed based on operational research [30], genetic algorithms [31,32] and stochastic optimisation [33,34]. Optimisation of a neighbourhood-scale cooling heating and electricity integrated energy network has been described in [35], where cooperative game-theory based constraints are proposed to model both cost and emissions' benefit allocation. The case study indicates that CHP plus heat pump can replace gas boilers for cost-efficient heating supply with significantly lower carbon emissions. A hierarchical approach for designing an integrated cooling, heating and electricity network at district scale is proposed in [33]. Fully distributed and semi-distributed design modes are compared from economic and computational efficiency perspectives and stochastic programming is used for modelling uncertainties.

Techno-economic approaches to planning of district heating and energy systems with detailed spatial resolution have been presented in [36,37], allowing for the optimisation of the routes and capacities of heat distribution networks, selecting heat loads that will be connected to a DHN and determining locations for the energy sources. A model of renewable energy-supplied DH in cities with integration of geospatial data of buildings and resources is presented in [38]. A rigorous optimisation-based clustering approach is used to reduce model complexity leading to a realistic DHN design aligned with the road network.

A decision support framework for the design of CHP-based combined DHN with boilers for peak load shaving has been presented in [39]. The model has been used to identify the optimal load ratio between the CHP and peak shaving boiler. The selection of technologies for the operation of a DH centre while considering hourly variations in electricity prices has been described in [40]. The integration of large-scale heat pumps into DHNs using low-temperature heat sources while considering seasonal variations in heat source temperature and the heat pump coefficient of performance has been modelled in [41]. The potential for deploying both long-term storage systems based on hydrogen and short-term storage systems based on batteries in decentralised neighbourhoods has been assessed in [42]. Estimating the demands and prices required by energy planning models is another important consideration. A linear regression model where the demand is calculated from the hourly weather data coupled with a social component and historical heat consumption data has been described in [43]. A bottom-up model of electricity costs that generates real-time price curves and provides profiles for different UK regions across various seasons has been presented in [44].

The integrated planning and operation of electricity and DHNs has been broadly investigated in literature. In [45], a network-constrained unit commitment (UC) model has been proposed for interconnected power and heat systems considering CHP units and DHNs. In this study, the heat storage system has been sized to match the intermittent wind power generation. An approach to risk analysis for optimal energy management of interconnected power and heat systems considering uncertainties associated with electricity price and wind power output was presented in [46], while in [47] an optimal robust energy management model for such integrated systems has been proposed to deal with uncertain parameters such as market price and loads, and in [48] the multi-objective optimisation of both system operation costs and emissions has been considered. In [49], a network-constrained optimal generation scheduling in interconnected power and heat networks has been studied in deterministic conditions. The uncertain nature of wind power output, load demand, and electricity market prices has been investigated from the aspect of energy management in [10] by applying a seasonal autoregressive integrated moving average model. A similar analysis has been carried out in [50] by employing a real-time management model that also included real-time market price signals.

A methodology to increase the efficiency and reduce cost of the power system by incorporating CHP in combination with thermal storage and DHN in energy systems has been proposed in [51], while considering the impact of the temperature of heat delivered by the CHP plant and of the DHN at whole energy system level, as well as including the feasible operating regions of CHP for different heat uses.

1.3. Novelty of proposed approach: Local and national interactions in DHN

Economic comparison of different heat decarbonisation pathways for the UK and the associated impacts on the electricity system were analysed in [2], suggesting that district heating may be economical in urban areas, in particular if its inherent flexibility is utilised to support the decarbonisation of the electricity system. Similarly, the whole-system modelling of the interaction between electricity and heat systems presented in [52] highlighted the benefits of system integration at both local and national level for cost-effective decarbonisation.

Most of the previous research on local district heating systems has focused on the local infrastructure, with only limited consideration of wider energy system impacts and benefits, which can be substantial, as demonstrated through whole-system approaches to integrated heat and electricity system assessment. In that context, the main contribution of this paper is to propose a novel optimisation framework for choosing a cost-efficient portfolio of heat supply technologies for a given local district heating system, while considering the interactions with a decarbonised electricity system at both national level and within the local

distribution grid. These interactions are implemented in a robust manner, by using input electricity price profiles derived from a whole-system model of the electricity system with varying shares of variable renewables. The proposed modelling approach allows for an explicit consideration of the impact of volatile electricity price patterns, resulting from factors such as increased penetration of renewables, local network constraints and limits on local carbon emissions. One of the key advantages of the approach proposed in this paper is to directly consider the interactions between heat and electricity networks and the associated impact on cost-optimal decisions to invest in heat generation assets as well as on their optimal operating strategies.

The proposed problem formulation will be integrated into the open-source application for heat network planning developed within the EU-funded THERMOS project [53]. The overall optimisation of a district energy system in THERMOS is decomposed into two separate models for the heat network and supply system respectively (Fig. 1). The heat network model determines the network paths for connecting individual buildings by optimising an objective function based on network investment costs, heat supply costs and revenues from heat sales [37]. The heat supply cost is a critical parameter in the heat network optimisation as it determines which connections are economically viable [36]. The supply system model described in this paper optimises this cost by exploiting the benefits of integrating heat and electricity networks.

Similar approaches to modelling district heating systems have been reported in the literature but differ in the level of detail and the optimisation strategy used to manage computational requirements for complex models. The supply system optimisation problem has been decomposed into a technology selection model and a detailed quarter-hourly operational simulation, which are optimised using iterative heuristic methods [54], however this analysis did not consider local grid constraints or electricity price volatility driven by renewables. A linear programming (LP) model application to optimise the capacity selection and hourly operation of the supply technologies over an entire year has been presented in [55], although without considering the specific impact of local grid constraints or electricity price variations. The impact of regulatory requirements, policy interventions and incentives such as feed-in tariffs has been included in the optimisation of the supply system assuming static electricity prices [56]. The modelling approach adopted in THERMOS combines a high spatial resolution MILP optimisation model for the heat network [37] with a high temporal resolution MILP optimisation model for the design and operation of the supply system described in this paper that incorporates volatile electricity price patterns and local network constraints.

2. Method

The interaction between heating (and potentially cooling) networks and the electricity grid occurs at both local and national scales. At the district level the circumstances in the local electricity distribution network and DHN will affect both the possibility and the cost of grid connection of a CHP plant or large-scale centralised HP. Local electricity network constraints could potentially limit the size of the connection or the rate of power consumption or injection that can be accommodated in the existing grid. Opportunities for connecting generation assets to the DHN with possible capacity limits, any planning regulations or network refurbishment constraints, heat demand intensity and future demand forecast will also have an influence on decisions to invest in heat networks. On the other hand, interactions with the wider energy system, in particular at bulk power system level, will be affected by time-varying prices of electricity, which will depend on the national generation mix and in particular on the contribution of intermittent renewable generation to the electricity supply. Highly fluctuating electricity prices will have an impact on the attractiveness of different heat supply options, including the installation of dedicated heat storage to increase the operational flexibility of power-to-heat technologies.

2.1. General approach

The model is formulated as a mixed-integer linear programming (MILP) optimisation problem, finding the solution that minimises the total cost of heat supply, including investment and operational costs, while considering specific constraints associated with local grid capacity and pollutant emissions.

Four types of heat supply sources are assumed: 1) Combined Heat and Power (CHP) plants, 2) large-scale centralised heat pumps (HP), 3) centralised boilers, and 4) thermal energy storage (TES). Each of these categories can accommodate a variety of technology subtypes and/or fuels such as gas or biomass boilers, fuel cells, engines or gas turbine as prime movers for CHP plants, or TES in the form of hot water tanks, molten salts or phase-change materials (PCMs).

Key links between the heat supply system (which is the subject of optimisation) and the electricity system include: a) CHP plants, which are able to sell their electricity output into the grid at the same time as supplying heat, and b) large HP plants, which produce heat from electricity purchased at time-varying prices. Fig. 2 illustrates the key interactions between heat and electricity distribution systems.

The model assumes a known annual heat demand profile, which for the sake of computational efficiency is represented as a set of daily

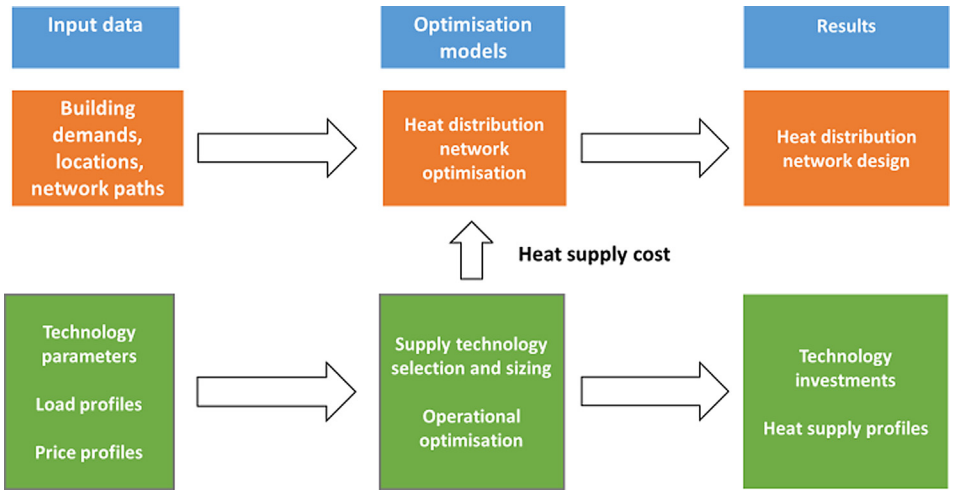

Fig. 1. Optimisation of district heat network and supply system.

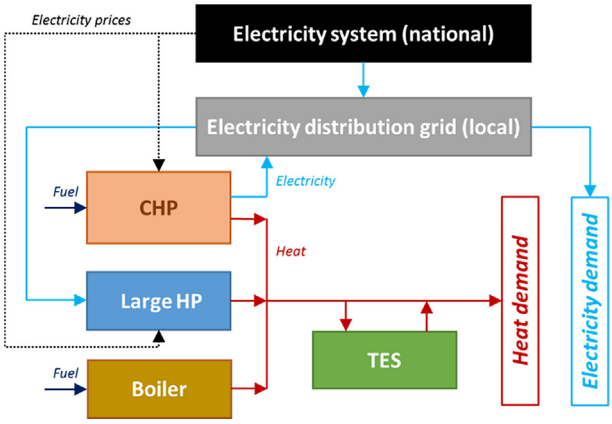

Fig. 2. Interactions between electricity system and heat supply system.

demand profiles for typical days and the associated frequencies of occurrence (e.g. representing peak winter day, normal winter day, spring/autumn and summer days; and/or workdays and weekends). The number of typical days is an input parameter into the model; the choice of typical days should capture the key seasonal variations in heat demand, electricity demand and electricity prices. It is assumed that the heat demand is supplied via a DHN that already exists and is therefore not the subject of optimisation.

2.2. Objective function

The objective function minimises the cost of supplying heat, considering the investment and operating cost components of the selected assets (including heat storage), and assuming it is possible to use an existing DHN. The main components of the objective function include:

- Investment cost into new CHP, large HP, heat storage and/or centralised boiler capacity
- Fuel cost of operating CHP and boiler plants
- Revenues from selling electricity generated by CHP
- Electricity purchase cost for large HP operation
- Cost of heat demand curtailment (if any)

The mathematical formulation of the objective function is provided in (1):

$$\begin{aligned} \min z = & \sum_{i=1}^{I} c_{CHP,i} + \sum_{j=1}^{J} c_{HP,j} + \sum_{k=1}^{K} c_{S,k} + \sum_{l=1}^{L} c_{B,l} + \Delta \cdot \sum_{d=1}^{D} N_d \\ & \sum_{t=1}^{T} \left(\sum_{i=1}^{I} (\omega_{CHP,i,t,d} - p_{CHP,i,t,d} \cdot B_{E,t,d}) + B_{E,t,d} \sum_{j=1}^{J} p_{HP,j,t,d} + \right. \\ & \left. \sum_{l=1}^{L} \frac{F_{B,l}}{\eta_{B,l}} \cdot h_{B,l,t,d} + C_{VOLL} \cdot h_{curt,t,d} \right) \end{aligned} \quad (1)$$

The first four terms in (1) represent the annualised investment cost components for CHP (c_{CHP}), HP (c_{HP}), TES (c_S) and boilers (c_B), respectively. This is followed by: the difference between the operating cost of CHP plants (ω) and the revenues from electricity sales represented as product of CHP power output (p_{CHP}) and electricity prices (B_E); cost of electricity used by HPs, expressed as product of HP power consumption (p_{HP}) and electricity prices (B_E); fuel cost of boilers, expressed as product of boiler heat output (h_B) and the ratio between the cost of fuel (F_B) and boiler efficiency (η_B); and the cost of heat demand curtailment (h_{curt}), penalised with a high cost coefficient C_{VOLL}. Δ represents the duration of the unit time interval (0.5 h is assumed in the examples presented later in the paper). The operating cost components are summed across all time intervals t and across all characteristic days d used in the study, weighted by their frequency of occurrence N_d. Therefore the total operating cost represents a weighted sum across all characteristic days, ensuring that the operating cost is adequately accounted for across the entire year and that it can be added to the annualised investment cost in the objective function. Note that any investment decisions in new supply capacity apply across all characteristic days in a year, as specified later in constraints (13)–(18).

It is assumed that DHN is already available to transport heat from the generation assets to the end users. There are a number of complexities associated with simultaneous optimisation of generation technologies and network design, including the different temporal and spatial resolutions required. Optimisation of generation/storage technologies generally requires a high temporal resolution, in particular to select the best operating strategies in light of dynamic system components response, operational flexibility, variable costs and emission levels and interactions with demand side management options, but it generally involves a relatively limited number of possible locations for technologies. On the other side, heat network design requires high spatial resolution, while in the time domain considering only peak and average heat demand is typically sufficient for optimising long-term investments. It is therefore more efficient to solve the two subproblems in an iterative fashion, with the heat supply optimised according to the method presented here, and network planning based on different approaches proposed in literature such as [37] or [57]. The heat generation asset optimisation therefore does not consider revenues from heat sales nor network investment/operational costs, but only capex and opex of heat generation and storage technologies.

The variable operating cost of CHPs and boilers can also include the cost of carbon emissions if relevant i.e. if the carbon price is relevant for the case study. Alternative objective functions (e.g. minimising carbon emissions) could be formulated with a similar approach, taking into account emission factors of CHP plants and boilers.

2.3. Model constraints

Constraints that need to be met in the model include:

- *Energy balance*. The total net heat output of all CHP (h_{CHP}), HP (h_{HP}), heat storage ($h_S^+ - h_S^-$) and boiler units (h_B) needs to meet the heat demand H in each time interval, also allowing for the possibility of curtailment (at a specified cost):

$$\sum_i h_{CHP,i,t,d} + \sum_j h_{HP,j,t,d} + \sum_k (h^+_{S,k,t,d} - h^-_{S,k,t,d}) + \sum_l h_{B,l,t,d} \geq H_{t,d} - h_{curt,t,d} \quad (2)$$

- *Investment costs*. The investment cost of new CHP (c_{CHP}), HP (c_{HP}), TES (c_S) and boiler units (c_B) is expressed as the sum of a fixed component I^F that is independent of the size (multiplied by binary investment variables u) and a variable component that is size-dependent and expressed as a product of parameter I^V and the continuous installed capacity variable π:

$$c_{CHP,i} \geq I^F_{CHP,i} \cdot u_{CHP,i} + I^V_{CHP,i} \cdot \pi_{CHP,i} \quad (3)$$

$$c_{HP,j} \geq I^F_{HP,j} \cdot u_{HP,j} + I^V_{HP,j} \cdot \pi_{HP,j} \quad (4)$$

$$c_{S,k} \geq I^F_{S,k} \cdot u_{S,k} + I^V_{S,k} \cdot \pi_{S,k} \quad (5)$$

$$c_{B,l} \geq I^F_{B,l} \cdot u_{B,l} + I^V_{B,l} \cdot \pi_{B,l} \quad (6)$$

- *Installed capacity limits*. New installed capacity of heat generators (π) is limited by the product of maximum capacity limits and binary investment decisions u, as defined in (7)–(10). In case the unit investment decisions are discrete, i.e. if one can only install the

specified maximum capacity or nothing, the inequalities in these constraints should be converted to equalities (all case studies presented later in this paper use inequalities i.e. allow continuous investment decisions).

$$\pi_{CHP,i} \leq u_{CHP,i} \cdot P^{MAX}_{CHP,i} \tag{7}$$

$$\pi_{HP,j} \leq u_{HP,j} \cdot P^{MAX}_{HP,j} \tag{8}$$

$$\pi_{S,k} \leq u_{S,k} \cdot H^{MAX}_{S,k} \tag{9}$$

$$\pi_{B,l} \leq u_{B,l} \cdot H^{MAX}_{B,l} \tag{10}$$

- *Operating cost of CHP*. The operating cost of CHP (ω_{CHP}) is composed of a fixed component independent of the delivered energy (no-load cost, NLC) and a variable cost component proportional to the CHP power output p_{CHP}; these two components are respectively defined for each unit as $A_{CHP,i}$ and $B_{CHP,i}$. NLC is incurred whenever the unit is operating but is not dependent on the unit output level. In standard unit commitment problems the NLC coefficient is typically expressed in € per operating hour for a unit of known size. However, given that the unit size is a decision variable and its value is not known in advance, the coefficient $A_{CHP,i}$ is here specified as 'unit' NLC in €/MW of CHP size and per operating hour. Parameters $A_{CHP,i}$ and $B_{CHP,i}$ are chosen so that the conversion efficiency loss at 50% of rated power output is 10%, which is a typical value reported in the literature for gas reciprocating engines, the technology considered in the proposed application [58]. In general, it can be shown that if Γ denotes the ratio of minimum to maximum CHP output, and Λ is the ratio of efficiencies at minimum and maximum output, the unit NLC coefficient $A_{CHP,i}$ can be expressed relative to the variable operating cost coefficient $B_{CHP,i}$ as in equation (11). For a known unit size the no-load operating cost of CHP at time t would be found by simply multiplying the relevant absolute NLC coefficient (in €/h) with the unit commitment variable for time t. This is however not possible in a mixed-integer linear problem when the unit size is not known in advance, as it would result in a product of two variables representing commitment and investment decisions i.e. in a non-linear constraint. Constraint (12) therefore ensures that the no-load cost is accurately accounted for while preserving the linearity of the formulation. If the CHP unit is switched on at time t, i.e. the binary unit commitment variable $\delta_{CHP,i,t,d}$ is equal to 1, the total operating cost is the sum of no-load and variable cost ($A_{CHP,i}\pi_{CHP,i} + p_{CHP,i,t,d}B_{CHP,i}$). If on the other hand the unit is switched off, the right-hand side of (12) takes a value that is less than or equal to zero, effectively resulting in zero operating cost.

$$A_{CHP,i} = \Gamma \cdot B_{CHP,i} \cdot \left(\frac{1-\Gamma}{\Lambda - \Gamma} - 1 \right) \tag{11}$$

$$\omega_{CHP,i,t.d} \geq A_{CHP,i} \cdot (\pi_{CHP,i} - (1 - \delta_{CHP,i,t,d}) \cdot P^{MAX}_{CHP,i}) + p_{CHP,i,t.d} \cdot B_{CHP,i} \tag{12}$$

- *Operating limits*. The outputs of CHP, HP, heat storage and boilers are limited by the relevant installed capacity decision variables as well as CHP unit commitment decisions, as specified in expressions (13)–(18). Constraint (15) ensures that if a CHP plant is turned on at time t (which is represented through binary commitment variables $\delta_{CHP,i,t,d}$), its output needs to be at or above the minimum level expressed relative to its installed capacity. Depending on the application, the model could also include more advanced operating constraints (especially for CHPs) associated with standard unit commitment problems, such as start-up costs, quadratic cost functions, ramping constraints, minimum up and down times etc.

$$p_{CHP,i,t.d} \leq \pi_{CHP,i} \tag{13}$$

$$p_{CHP,i,t.d} \leq \delta_{CHP,i,t,d} \cdot P^{MAX}_{CHP,i} \tag{14}$$

$$p_{CHP,i,t.d} \geq \Gamma^{min}_{CHP,i} \cdot \pi_{CHP,i} + P^{MAX}_{CHP,i} (\delta_{CHP,i,t,d} - 1) \tag{15}$$

$$p_{HP,j,t,d} \leq \pi_{HP,j} \tag{16}$$

$$h^{+}_{S,k,t,d},\ h^{-}_{S,k,t,d} \leq \pi_{S,k} \tag{17}$$

$$h_{B,l,t,d} \leq \pi_{B,l} \tag{18}$$

- *Heat storage balance*. The duration parameter for heat storage is defined as the ratio between its energy (MWh) and power (MW) rating. Similar to CHP, HP and boiler units the investment cost of TES is expressed per unit of power. It would be equivalent to express the cost per unit of TES energy capacity and then express its power rating in MW as the ratio between energy and duration. The state of charge (SoC) or energy content of heat storage at time t ($w_{S,k,t,d}$) is equal to the SoC at time $t-1$ plus the net effect of charging ($h^{+}_{S,k,t,d}$) and discharging ($h^{-}_{S,k,t,d}$), multiplied by the duration of the unit time interval Δ, while also accounting for roundtrip losses $\eta_{S,k}$ (19). SoC is also limited from above by the product of thermal power rating ($\pi_{S,k}$) and duration of heat storage $D_{S,k}$ as specified in (20), and from below using the minimum relative SoC parameter W^{min} as in (21):

$$w_{S,k,t,d} = w_{S,k,t-1,d} - \Delta \cdot (h^{+}_{S,k,t,d} - \eta_{S,k} \cdot h^{-}_{S,k,t,d}) \tag{19}$$

$$w_{S,k,t,d} \leq \pi_{S,k} \cdot D_{S,k} \tag{20}$$

$$w_{S,k,t,d} \geq W^{min}_{S,k} \cdot \pi_{S,k} \cdot D_{S,k} \tag{21}$$

- *Heat to power ratios*. Power generation/consumption and heat production for CHPs and HPs are linked via proportionality constraints that feature the ratios R_{CHP} for CHP and R_{HP} that represents the COP of the heat pump (note that both of these are assumed to be time-independent, but could easily be replaced by temporally varied profiles):

$$h_{CHP,i,t,d} = R_{CHP,i} \cdot p_{CHP,i,t,d} \tag{22}$$

$$h_{HP,j,t,d} = R_{HP,j} \cdot p_{HP,j,t,d} \tag{23}$$

- *Local electricity grid*. Constraints associated with the local power network (assuming any CHP plants or large HPs would be connected to the same network substation) need to ensure that the aggregate effect of baseline power demand (D), CHP generation and HP consumption does not exceed substation capacity G_{cap} (24). This constraint also accounts for limits on any reverse power flows (i.e. power injections into the grid) using a coefficient $\alpha < 1$, given that for technical reasons the substations can normally accommodate slightly lower power flows in the reverse than in the default direction.

$$-G_{cap} \cdot \alpha \leq D^{el}_{t,d} + \sum_{j} p_{HP,j,t,d} - \sum_{i} p_{CHP,i,t,d} \leq G_{cap} \tag{24}$$

- *Carbon emission constraints*. Total annual carbon dioxide (CO_2) emissions (or in a more general case CO_2-equivalent emissions of greenhouse gases) from the heat supply system can be constrained so as not to exceed a pre-specified annual limit. Carbon emissions can result directly from the operation of CHP plants and boilers, quantified by multiplying their respective outputs with relevant emission factors E_{CHP} and E_B, or indirectly as the carbon emissions associated with grid electricity ($E^{gridCO_2}_{t}$) used to operate HPs:

$$\Delta \cdot \sum_{d=1}^{D} N_d \sum_{t=1}^{T} \left(\sum_{i=1}^{I} p_{CHP,i,t,d} \cdot E_{CHP,i} + \sum_{j=1}^{J} p_{HP,j,t,d} \cdot E^{gridCO_2}_{t} + \sum_{l=1}^{L} h_{B,l,t,d} \cdot E_{B,l} \right) \leq E_{CO_2} \tag{25}$$

- *Local emission constraints*. Total annual emissions of nitrogen oxides (NO_x) and particulate matter (PM) from CHP plants and boilers can also be constrained so as not to exceed a pre-specified emission limit for the heat supply system:

$$\Delta \cdot \sum_{d=1}^{D} N_d \sum_{t=1}^{T} \left(\sum_{i=1}^{I} p_{CHP,i,t,d} \cdot E_{CHP,i}^{NO_x} + \sum_{l=1}^{L} h_{B,l,t,d} \cdot E_{B,l}^{NO_x} \right) \leq E_{NO_x} \quad (26)$$

$$\Delta \cdot \sum_{d=1}^{D} N_d \sum_{t=1}^{T} \left(\sum_{i=1}^{I} p_{CHP,i,t,d} \cdot E_{CHP,i}^{PM} + \sum_{l=1}^{L} h_{B,l,t,d} \cdot E_{B,l}^{PM} \right) \leq E_{PM} \quad (27)$$

The model has been implemented in the FICO Xpress optimisation software [59] in order to produce the case study results presented in the next section.

2.4. Common assumptions

The assumptions used in these examples are for illustration only and are not intended to be representative of a specific technology or location. For simplicity, all case studies assume that only one unit of each technology (gas-fired CHP, large-scale HP, TES and gas-fired boiler) is available for installation.

In single-day case studies presented in Sections 3.1–3.4, only one characteristic day was assumed to represent the heating season, with 48 half-hourly intervals for heat demand values. It was further assumed that this day repeats 150 times during a year (representing the length of the heating season), that the heating system is only providing space heating, and that no heating (such as e.g. hot water) is required from the DHN during the rest of the year. On the other hand, in multiple-day examples presented in Section 3.5, it was assumed the heating season can be adequately represented using 3 characteristic days. No cooling demand was considered.

2.4.1. Investment cost and installed capacity limits

Default assumptions used in case studies for annualised investment cost and maximum installed capacities are presented in Table 1. Annualised investment costs are obtained from overnight investment costs by applying the discount rate of 5% and assuming 15 years as the economic life of assets. Note that in some case studies the input parameters from Table 1 were varied to evaluate their impact on the optimal solution.

Note that making accurate cost estimates of heat supply technologies is not the main objective of the paper, especially since some of these cost parameters are varied significantly across the examples presented in this paper in order to assess their impact on the optimal solution. Nevertheless, the investment costs are assumed to be of the correct order of magnitude compared to those proposed in the relevant literature [60]. Given the sizes of CHP units considered (up to 2 MW_{el}) the most suitable choice of CHP technology is likely to be a reciprocating gas engine. For the HP considered here (in the megawatt-scale) we assume that this is a ground-source or water-source HP based on a vapour-compression cycle. The assumptions for boilers are broadly consistent with a natural gas-fired boiler.

The variable CHP operating cost component per unit of electricity output was assumed to be €80/MWh. Single-day examples presented in Sections 3.1–3.4 assumed the values for NLC coefficients and minimum output to be zero, effectively making the unit commitment decisions irrelevant. In contrast, in the multiple-day examples presented in Section 3.5 the assumed unit NLC coefficient was €10/MWh, ensuring a 10% efficiency loss at minimum output level, assumed to be at 50% of maximum output. The fuel (i.e. gas) cost for operating the boiler was assumed at €30/MWh, and its efficiency was 95%. The emission factor per unit of output for CHP was 0.5 tCO_2/MWh_{el}, and for boilers 0.2 tCO_2/MWh_{th}. No specific cost of carbon was assumed.

The assumed heat-to-electricity (H-E) ratio for CHPs was 2.0, which is in line with the range of 1.1–2.5 for reciprocating engines reported in [61] (the value of 2.0 was chosen to ensure sufficient heat output from the CHP to supply heat demand). The Coefficient of Performance (COP) for large-scale HPs was assumed to be 3.0, which is in line with typical values reported in the literature [60]. Given that a constant COP value is used, the influence of variations in environmental temperature and building comfort parameters or indoor temperature on the COP variation has not been considered in this work; however, it would be straightforward to include temporal variations in COP if relevant. Heat storage duration (ratio between rated energy and power) was assumed to be 4 h, the minimum SoC was set at 0% and the assumed roundtrip efficiency of TES was 90%.

2.4.2. Electricity price profiles

A number of daily electricity price profiles has been assumed in the proposed case studies, as illustrated in Fig. 3, reflecting different penetrations of intermittent renewable energy that may influence the planning and operation of heat generation technologies. Note that the price profiles are only illustrative examples, and not all of them would be likely to be sustained over the course of the heating season. Price profiles presented here are used in single-day examples presented in Sections 3.1–3.4; multiple-day examples in Sections 3.5 and 3.6 used different profiles, as elaborated in those sections.

The profiles include:

- *Flat*: Fixed electricity price profile (€50/MWh) throughout the day. It can also represent a scenario where a power purchase agreement (PPA) is signed by a CHP or a large HP operator.
- *Variable*: Variable electricity price profile for a typical day, varying between €36/MWh (overnight) and €65/MWh (peak demand hours).
- *Low Peak*: Price scenario reflecting a downward pressure on prices during peak hours due to abundant wind generation (being a plausible scenario for the UK system).
- *Extreme Peak*: A future price scenario that reflects scarcity pricing, pushing the electricity prices to a very high level during peak demand periods as the result of high demand levels and low renewable (wind) generation.

2.4.3. Heat and electricity demand

Heat demand profile for the single characteristic day used in case studies of Sections 3.1–3.4 is shown in Fig. 4, with a peak demand of about 2.5 MW_{th}, corresponding to a large block of buildings or a small borough in an urban area. Baseline electricity demand profile at the local substation (before including the impact of the local heating system i.e. without any power generation or consumption by CHP and HP installations) was assumed to follow the pattern also depicted in Fig. 4 (right-hand vertical axis), with peak demand level just above 3 MW_{el}. The capacity of the local electricity substation was assumed to be 4 MW_{el}.

Table 1
Assumptions on investment cost and maximum capacities for heat supply technologies.

Parameter	*Technology*			
	CHP	Large HP	TES	Boiler
Fixed cost (€/yr)	5000	10,000	1000	2000
Variable cost (€/kW/yr)	50	100	10	20
Max. capacity (MW)*	2	2	5	5

* Note: Capacities of CHP and large HP are expressed as electrical power (in MW_{el}), while those of TES and boilers refer to thermal capacities (in MW_{th}). These limits are chosen on the basis of the heat demand profile of the selected case study.

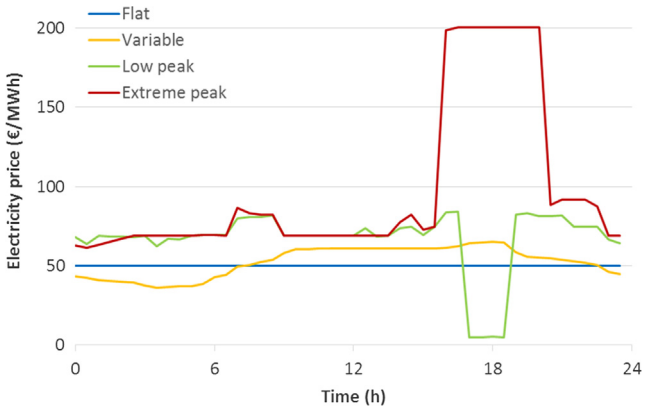

Fig. 3. Electricity price profiles used in case studies.

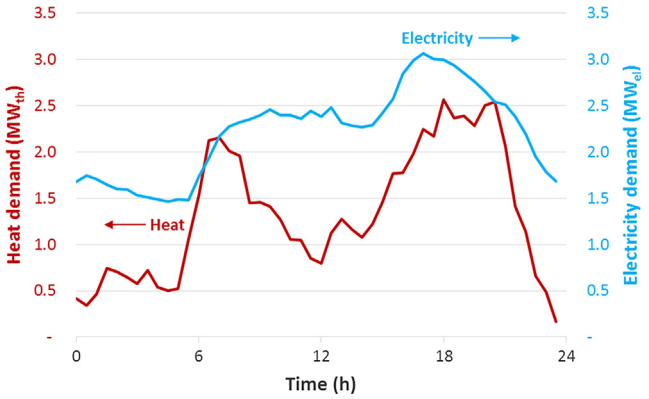

Fig. 4. Daily heat demand and local electricity demand profiles.

3. Results and discussion

The proposed model was applied to a number of representative case studies that highlight the capability of the model to address cost-efficiency trade-offs for a portfolio of heat generation technologies including the interaction between heat and electricity systems. Sections 3.1–3.4 present the application of the model to case studies with a single representative day, while Sections 3.5 and 3.6 present examples with multiple representative days.

Table 2 provides a description of the proposed case studies for the single-day analysis, with related assumptions for the investment costs. A total of 8 single-day case studies have been proposed to illustrate the impact of the following key drivers on investment decisions: 1) electricity price profiles, 2) investment cost of heat supply technologies, 3) constrained electricity network capacity, and 4) constrained carbon emissions. The assumptions for multiple-day case studies are specified in Sections 3.5 and 3.6.

Key model outputs for each case study include: a) installed capacities of CHP, HP, thermal storage and boilers, b) total annual cost of supplying heat, and c) average cost of heat supplied to customers. The results for installed capacities for CHP and HP refer to their electrical power (in MW_{el}), while those for TES and boilers refer to thermal capacities (in MW_{th}).

3.1. Variations in electricity prices

3.1.1. Flat price profile

Fig. 5 shows the daily diagram of heat supply and demand for the *Flat* electricity price profile (shown in Fig. 3), as well as the optimal investment choices for heat sources.

The cost-optimal supply mix in this case is achieved by a mix of 0.7 MW_{el} of CHP and 1.23 MW_{th} of heat storage. This combination allows the CHP plant to operate at almost constant output, producing around 1.4 MW_{th} of heat. The remaining heat demand during peak periods is matched by heat stored in the TES, and this heat is then replenished during off-peak periods, while still allowing CHP to operate at full output. Despite the flat electricity prices seen by the CHP plant, it is still justified to build some heat storage alongside the CHP. Building any additional CHP capacity above the optimal 0.7 MW_{el} would reduce its utilisation factor and make the total cost higher than for the combination of CHP and TES.

CHP produces electricity at €80/MWh_{el} while earning a revenue of €50/MWh_{el}. The difference of €30/MWh_{el}, when applied to the 2 MWh of heat produced simultaneously with 1 MWh of electricity results in a net heat cost of €15/MWh_{th}. The heat generation cost of large HPs, assuming the COP of 3, would be €16.7/MWh_{th}, which combined with a higher investment cost of HPs explains why CHP is preferred. Gas boiler on the other hand can produce heat at €30/MWh, which is significantly higher than CHP, so even the lower investment cost of boilers does not justify choosing them as a supply source. The average cost of supplying heat in this example, after accounting for all operating costs as well as the investment cost of CHP and heat storage capacity, is around €26/MWh_{th}.

Daily changes in the State of Charge (SoC) of TES are shown in Fig. 6. A positive gradient of SoC is observed during off-peak periods, when TES is charged with heat produced by the CHP in excess of current heat demand, while negative gradients occur during peak demand periods when heat storage output is used to top up the heat supplied by the CHP. The model ensures that TES is fully charged before the beginning of morning and evening peaks.

3.1.2. Time-varying price profiles

The impact of other electricity price profiles (Variable, Low Peak and Extreme Peak) on investment decisions, total net annual cost and daily diagrams of heat supply is shown in Fig. 7.

The cost-optimal mix of heat sources with Variable electricity prices (Fig. 7a) includes more CHP capacity (0.87 MW_{el}) and less TES capacity (0.84 MW_{th}) than with Flat prices. The overall net cost decreases by 8%, with the average heat supply cost of €24.2/MWh_{th}. Although the peak heat demand still requires both CHP and TES to be used, higher CHP capacity allows it to run at higher output during high price periods. TES is mostly charged during the mid-day low-demand hours and late evening, and this heat is again released to help meet the morning and evening peak demand. The CHP operates at a lower level during the night when the electricity prices and hence the available net revenues are lower.

The scenario with Low Peak electricity prices (Fig. 7b) emulates a price drop during peak demand periods, e.g. due to high output of wind generation, while outside these periods the prices are relatively higher (Fig. 3). The optimal volume of CHP capacity is similar to Flat prices scenario (0.71 MW_{el}), but the optimal TES capacity is now higher (1.50 MW_{th}). Thanks to high electricity prices outside the peak demand

Table 2
Overview of main assumptions across single-day case studies.

No.	Electricity price profile	CHP cost	TES cost	Boiler cost	Network constraint	CO_2 constraint
1	*Flat*	Default	Default	Default	–	–
2	*Variable*	Default	Default	Default	–	–
3	*Low Peak*	Default	Default	Default	–	–
4	*Extreme Peak*	Default	Default	Default	–	–
5	*Flat*	4x higher	Default	Default	–	–
6	*Flat*	Default	10x higher	2x lower	–	–
7	*Flat*	4x higher	Default	Default	Active	–
8	*Flat*	Default	Default	Default	–	Active

Note: 'Default' investment cost assumptions (fixed and variable) are given in Table 1.

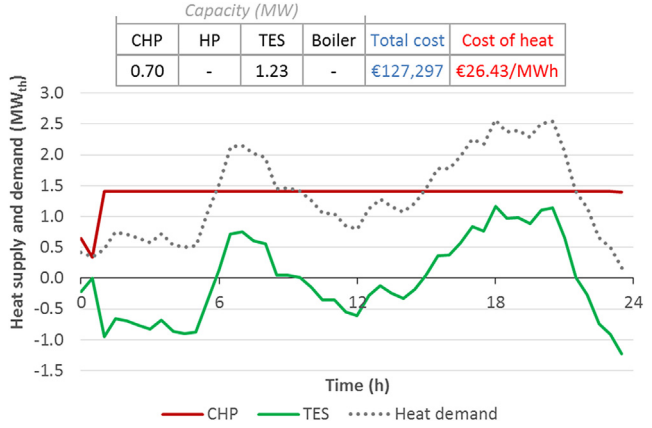

Fig. 5. Heat supply profile and investment decisions for *Flat* electricity prices.

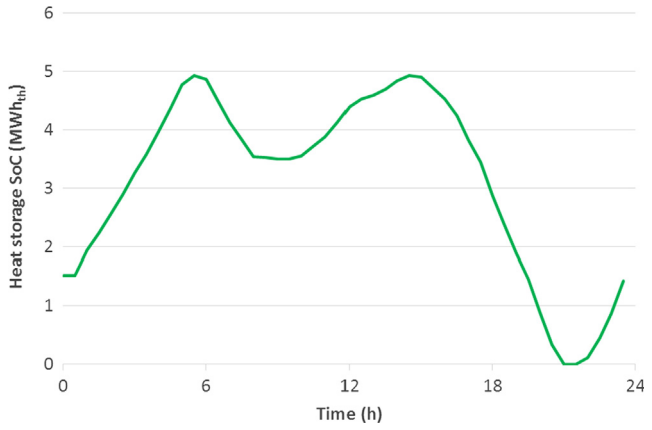

Fig. 6. Daily variation of energy stored in TES.

window, the overall net cost of heat supply is significantly lower than in previous case studies, with the average cost of heat of only €17.4/MWh. In the daily diagram CHP operates at full output outside the low-price window, taking advantage of relatively high electricity prices compared to its operating cost. Conversely, when power prices drop between 5 pm and 6.30 pm, the CHP operation is no longer profitable, and hence most of the heat in that period is released from TES.

Finally, in the Extreme Peak price scenario (Fig. 7c), acknowledging the low likelihood of such a scenario persisting over the entire heating season, the optimal solution includes only CHP capacity at the maximum allowed level of 2 MW_{el}. Due to extremely high revenues from selling power, the net annual cost of supplying heat becomes negative in this example (–€11.8/MWh_{th}). Note that this scenario assumes that heat dumping is allowed i.e. that any heat produced by CHP in excess of actual heat demand could be released into the environment if economically justified. This is also reflected in constraint (2) that is formulated as inequality rather than equality. (Had the option for heat dumping been disabled, CHP would be installed at the level of 1.28 MW in order to meet peak heat demand, while the net cost of heat would be –€3.3/MWh_{th}.) The CHP operating strategy in this case is to produce heat equal to the demand if the electricity price is below its operating cost (€80/MWh), and operate at maximum output if the price exceeds €80/MWh, while dumping any excess heat.

3.2. Sensitivity to investment cost assumptions

Fig. 8 shows the investment decisions, net annual cost and daily diagrams of heat supply for case studies with high CHP investment cost (case #5 in Table 2), and high CHP and TES but low boiler cost (case #6 in Table 2).

Higher investment cost of CHP (Fig. 8a) changes the optimal technology mix, now consisting of 0.47 MW_{el} of large-scale HP capacity and 1.23 MW_{th} of TES. This also results in about 20% higher total net cost and the average cost of heat of €31.6/MWh_{th}. Daily operating patterns of HP and heat storage are similar to Fig. 5, except that the 1.4 MW_{th} of baseload heat is now supplied by large-scale HP. This also means that the local electrical substation will see an increase in electricity demand, including an increase in peak demand by 0.5 MW_{el} (which is still below the assumed substation rating of 4 MW).

With higher CHP cost combined with higher TES cost and lower boiler cost (Fig. 8b) the optimal solution no longer includes heat storage, but a combination of a large HP (0.47 MW_{el}) and boiler (1.16 MW_{th}). The total annual net cost is now about 8% higher than in Fig. 8a, and the average cost of heat is €34.1/MWh_{th}. In the daily heat supply diagram the HP supplies heat demand up to the level of 1.4 MW_{th}, and gas boiler tops up the HP output whenever the heat demand exceeds this level.

3.3. Constraints in local electricity grid

This example considers the interdependencies with the local electricity network by assuming that in addition to the assumptions made in case #5 there is a constraint on total active power that can be supplied through the local substation, at the level of 3.2 MW_{el}. This means that the large HP can no longer be operated in the same way as in Fig. 8a, as this would overload the substation during peak demand hours. The optimal solution, shown in Fig. 9a, includes a similar volume of large HP capacity as before (0.50 MW_{el}), but a significantly higher volume of TES (1.97 MW_{th}), which allows for the HP output during peak hours to be partly replaced by heat released from TES. The local grid constraint gives rise to a 7% net cost increase, with the resulting cost of heat of €33.9/MWh_{th}. Daily output diagram for this case shows that higher TES capacity is required to enable HP output to reduce sufficiently during the evening peak (from 4 pm to 7.30 pm) to avoid overloading the local electrical substation.

The loading profile for the local substation is presented in Fig. 9b. The power demand of large HP is reduced during the peak period in order to maintain the aggregate substation loading (baseline demand plus HP consumption) at the level of substation capacity (3.2 MW_{el}). In this case it becomes justified to increase the size of TES beyond the requirement of the heat network itself in order to ensure a more flexible interaction between the district heating system and the local electricity grid.

3.4. Constraints on carbon emissions

Case #8 is the same as case #1 except that it has an explicit limit on annual carbon emissions from the heat supply system, at the level of 500 tCO_2. Fig. 10 shows the daily heat supply pattern and optimal investment decisions for this scenario.

Only gas-fired CHP and boilers were assumed to be direct CO_2 emitters, while large HPs were not assumed to produce any direct emissions and the grid carbon intensity was also assumed to be zero. Without the emission constraint (case #1) the optimal solution only included CHP and TES capacity, and the resulting annual carbon emissions from the CHP were 1230 tCO_2. Restricting the carbon emissions, however, limits the output that can be provided by the CHP, and therefore its capacity is reduced from 0.7 to 0.3 MW_{el}. To compensate for that, the model adds about 0.27 MW_{el} of large HP capacity. Instead of CHP continuously providing 1.4 MW_{th} of heat on its own as in case #1, the heat output is now split between CHP (0.6 MW_{th}) and large HP (0.8 MW_{th}). If the carbon constraint is tightened further, even more of the low-cost CHP will be replaced by higher-cost HP (at zero-carbon target all CHP capacity would be replaced by HPs).

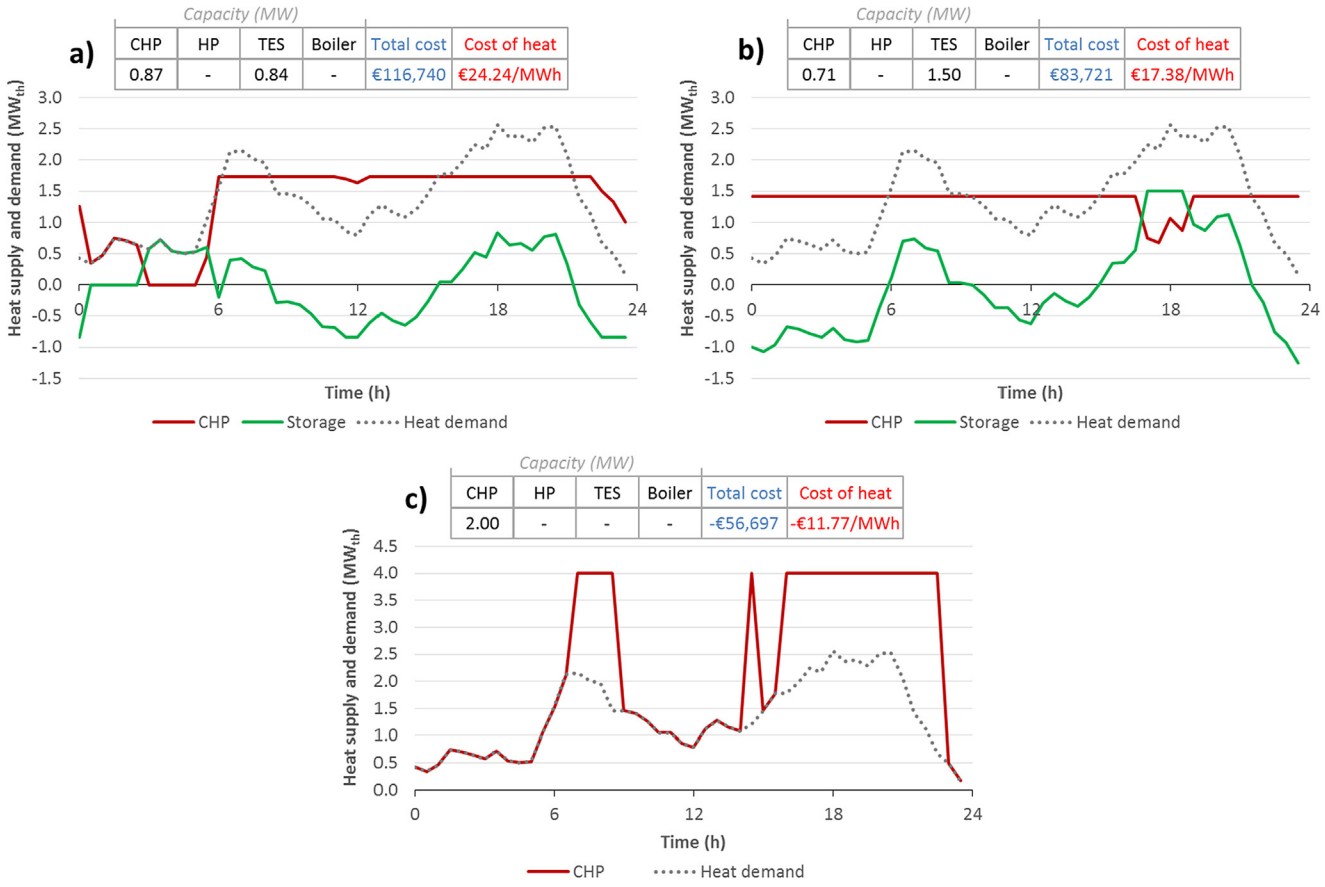

Fig. 7. Heat supply profiles and investment decisions for a) Variable, b) Low Peak and c) Extreme Peak electricity prices.

3.5. Multiple representative days

The next set of examples presented in this section is based on more detailed modelling of CHP operation and the seasonal variations of heat demand and electricity prices. For the examples presented in this section it is assumed that the heating season can be adequately represented using 3 representative days: a) winter peak, b) winter average and c) autumn/spring average day. These three days are assumed to occur with the following respective frequencies over the course of a year (N_d): 5, 60 and 85 (making the total duration of the heating season equal to 150 days, as in single-day examples). Daily heat demand diagrams used for the 3 representative days are shown in Fig. 11.

Electricity price profile for the spring/autumn average day was assumed to correspond to the Variable profile from Fig. 3. Price profiles for winter peak and winter average days were scaled up from the Variable profile using the scaling factors of 1.5 and 1.1, respectively.

Assumptions on CHP plants have been modified compared to those described in Section 2.4.1 so that a unit NLC coefficient $A_{CHP,i}$ was assumed to be €10/MWh, and the minimum output coefficient $\Gamma^{min}_{CHP,i}$ was assumed to be 0.5. Unlike in the single-day examples where the unit commitment decisions were effectively irrelevant due to zero values assumed for $A_{CHP,i}$ and $\Gamma^{min}_{CHP,i}$, the unit commitment decisions now have a direct effect on the solution.

The application of the proposed model with multiple characteristic days is demonstrated for three case studies:

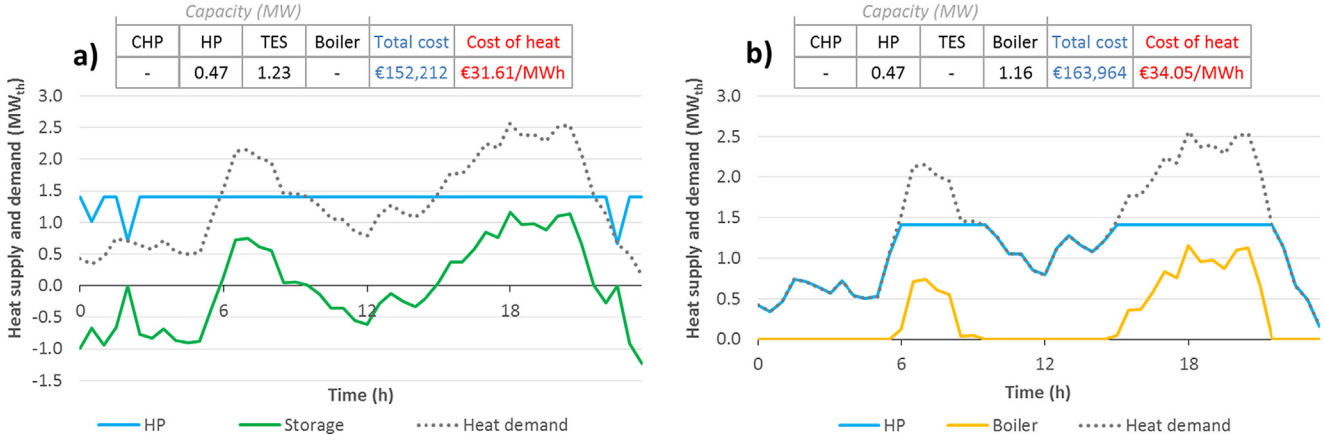

Fig. 8. Heat supply profiles and investment decisions for a) high CHP cost (case #5) and b) high CHP, high TES and low boiler cost (case #6).

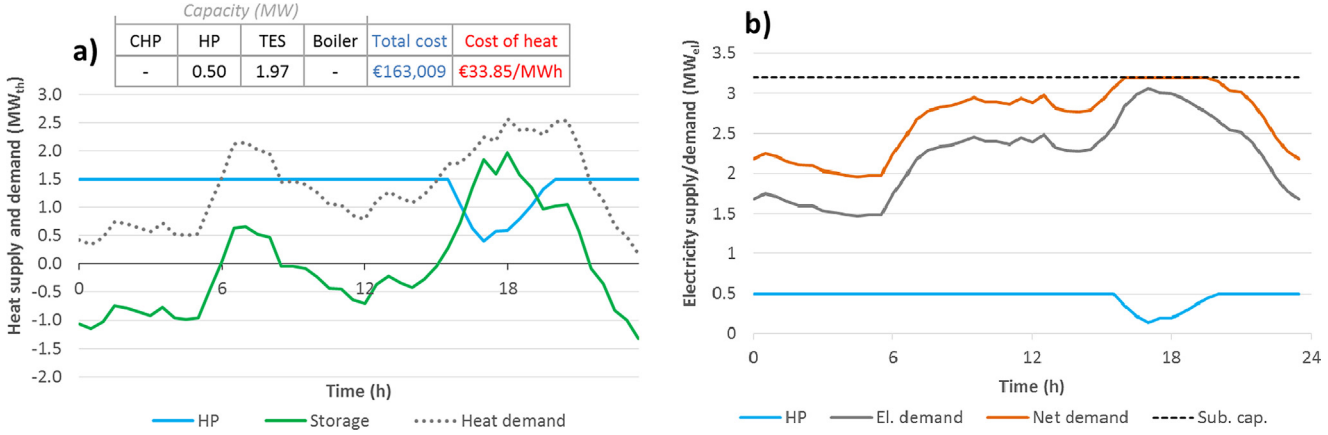

Fig. 9. a) Heat supply profiles and investment decisions, and b) electricity demand profile at local substation for high CHP cost and constrained local grid (case #7).

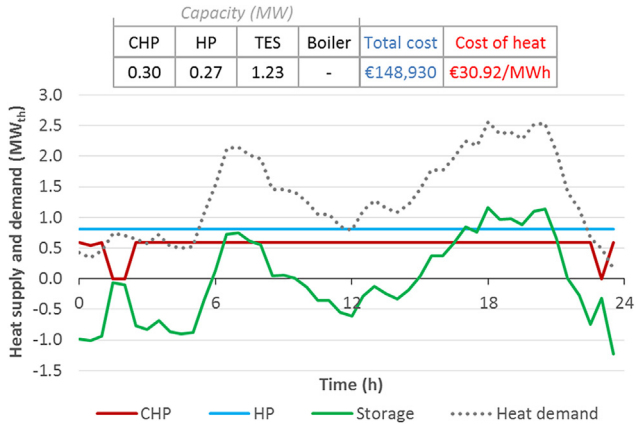

Fig. 10. Heat supply profiles and investment decisions with constrained carbon emissions.

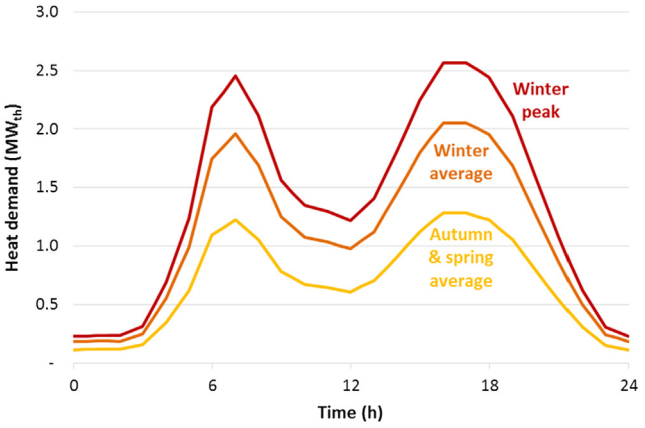

Fig. 11. Heat demand profiles for multiple-day example.

- Original set of assumptions from Table 1 and Section 2.4.1 without emission or grid constraints (Case A)
- Imposing a zero carbon constraint (Case B)
- Zero carbon constraint with constrained grid (Case C)

3.5.1. Unconstrained case study

The cost-optimal solution in Case A is to install 0.85 MW_{el} of CHP capacity and 0.87 MW_{th} of TES capacity. The resulting heat supply diagrams for the 3 characteristic days are given in Fig. 12. The operating strategies of CHP and TES units adapt to the level of heat demand and electricity prices over the course of the year. During the winter peak day (Fig. 12a), the CHP unit is operating at maximum output of 1.7 MW_{th} through most of the day, only being switched off between 1.30am and 4am, when the demand level as well as electricity prices are low and due to part-load efficiency losses it is not attractive to keep the unit operating at low output. TES is used to supply additional heat during morning and evening peaks as well as while the CHP unit is off, while outside of those periods TES absorbs excess heat produced by the CHP unit. On a winter average day (Fig. 12b) CHP still operates at full output, but for a shorter time, between about 6am and 9 pm, which is when the heat demand is the highest. TES is again used to top up extra heat during morning and winter peaks and supply heat while CHP is not in operation. Finally, during the spring/autumn day (Fig. 12c) the CHP unit is turned on twice during the day, between 6am and 10am to meet the morning peak and between 1.30 pm and 7.30 pm to meet the afternoon/evening peak.

The resulting average cost of supplying heat for Case A is €32.6/MWh_{th}, while the annual carbon emissions amount to 828 tCO_2, as it was assumed that the CHP unit uses natural gas. In the context of heat decarbonisation this may not be viable in the long term; therefore the next case study explores the options to deliver low-carbon heat.

3.5.2. Carbon constraint on heat supply

In Case B it was assumed that the heat supply system should have zero carbon emissions. In order to make this case study compatible with the objective to decarbonise national electricity supply as well, it was assumed that the carbon intensity of grid electricity was zero. The cost-optimal portfolio for Case B includes 0.49 MW_{el} capacity of large HP and 1.75 MW_{th} of TES capacity. Daily heat supply diagrams for three representative days are shown in Fig. 13. On winter peak days the HP operates at maximum output throughout the day (Fig. 13a), while TES is releasing heat during peak periods and absorbing it during off-peak periods, effectively following the shape of the heat demand diagram. On a winter average day (Fig. 13b) the HP operates at full output during the night i.e. from about 10 pm to 8am, taking advantage of lower electricity prices to store excess heat into TES. HP output then follows the heat load around midday and reduces to almost zero during the evening peak, triggered by higher electricity prices, while TES supplies heat at maximum capacity during the evening peak. A similar pattern is observed for the spring/autumn day (Fig. 13c), with TES supplying almost the entire heat demand during highest price periods.

The zero-carbon solution for heat supply presented in Fig. 13 increases the unit cost of heat delivered to customers to €41.9/MWh_{th}, which is 28% higher than in Case A. Another important consideration is that the operation of large HP imposes additional load on the local distribution substation. This is particularly relevant for the operation on a winter peak day, which is also when peak electricity demand is normally observed in distribution grids. The additional electricity demand

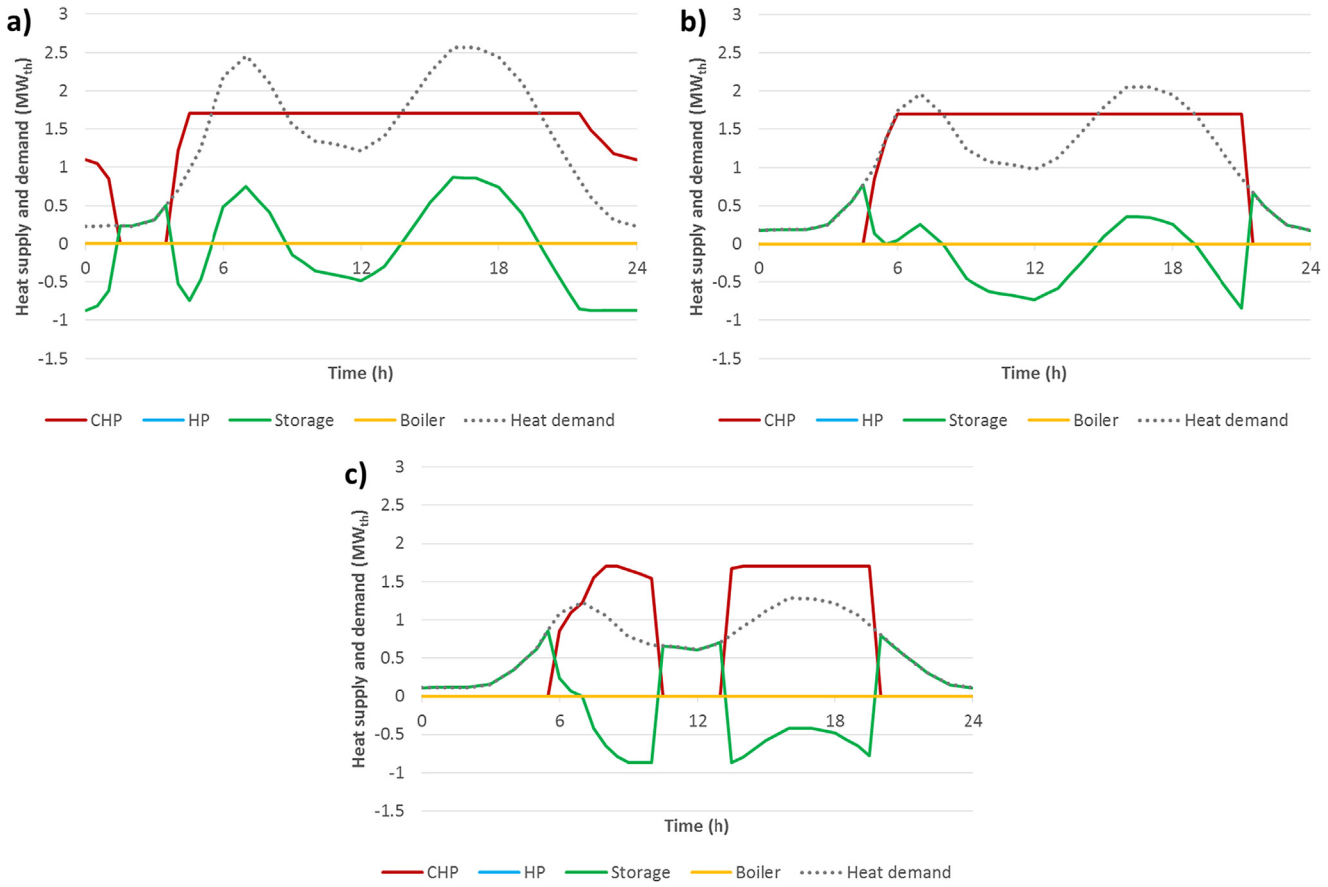

Fig. 12. Heat supply profiles in Case A for: a) winter peak, b) winter average and c) spring/autumn average day.

for HP operation, equal to about 0.5 MW_{el} during the winter peak day, could potentially overload the local distribution network. Given the baseline peak demand at the local substation assumed at 3.07 MW_{el} (Fig. 4), the total peak loading of the substation during winter peak day increases to 3.55 MW_{el} as the result of HP operation.

3.5.3. Carbon emission limit and local grid constraint

In order to simulate the conditions in which the additional HP demand would potentially overload the substation transformers, it is assumed in Case C (similar to the case study presented in Section 3.3) that the loading of the local substation is limited to 3.2 MW_{el}. The optimal investment decisions for this case include 0.53 MW_{el} of large HP capacity and 2.16 MW_{th} of TES capacity. Compared to Case B, there is a very slight increase in optimal HP capacity, but on the other hand a considerable expansion of TES capacity, by about 24%. Daily heat supply diagrams across different seasons as well as the resulting total loading of the local substation are presented in Fig. 14. The key change compared to Case B is the HP operation pattern during winter peak day (Fig. 14a), where the HP output reduces during peak hours to ensure that the total loading of the local substation does not exceed the 3.2 MW limit (Fig. 14d). To ensure that the heat demand is met during peak hours, heat is released from TES at up to its maximum output of 2.16 MW_{th}, which also explains why more TES capacity is needed in Case C than in Case B.

Imposing an additional constraint driven by the limitations in the local distribution grid is also reflected in an increased average cost of heat, which in Case C rises to €44.2/MWh_{th} or about 5% above the cost in Case B and 35% higher than in Case A.

3.6. Impact of variations in renewable penetration

The final set of case studies presented in this section explores the impact of variations in electricity prices driven by increasing penetration of variable renewable energy sources (RES), such as wind or solar PV generation, on investment and operation decisions for heat sources supplying the DHN. In order to simulate electricity price profiles that are linked to RES penetration, annual system marginal prices (SMPs) have been extracted from a whole-system model for the future GB electricity system described in [62]. Two systems with different shares of variable RES output have been considered: 1) a Low RES share system with 35% share of variable RES in electricity supply; and 2) a High RES share system with RES share of 63% (for reference, the 2019 share of variable RES in GB electricity supply was around 24%).

For the purpose of this section it was assumed that the heating season includes winter, spring and autumn. Based on the SMP outputs of the whole-system model, typical electricity price patterns have been constructed for six representative days:

- Winter peak day
- Winter average day
- Autumn day with low RES output
- Autumn day with high RES output
- Spring day with low RES output
- Spring day with high RES output

The corresponding daily price profiles for the six days are shown in Fig. 15 (frequencies of occurrence of typical days over the heating season are indicated in brackets alongside day labels). Winter peak profile is constructed in order to adequately consider the requirements for peaking capacity of heat production. RES output was found to have

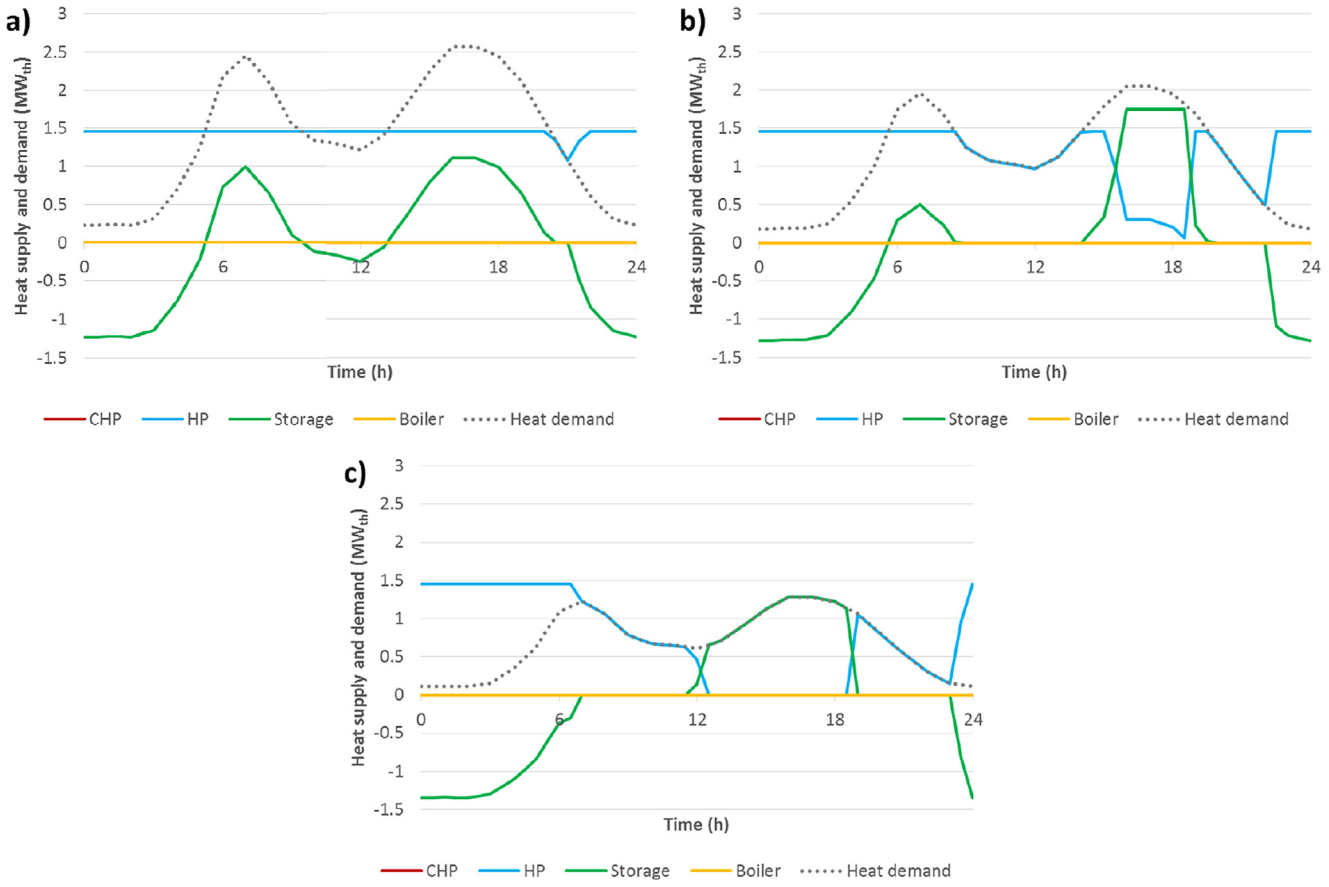

Fig. 13. Heat supply profiles in Case B for: a) winter peak, b) winter average and c) spring/autumn average day.

little impact on price levels during average winter days, therefore only one winter average day type is used. On the other hand, during spring and autumn, a distinction is made between days with relatively high RES output (also reflected in price levels) and those with low to average RES output. The volatility of prices on high RES output days reflects the level of RES penetration: in the low RES share system prices for those days tend to be visibly lower but still positive, while in the high RES share system there are periods of negative prices suggesting surplus RES output. In spring these periods coincide with high PV output around mid-day, while in autumn negative prices occur during low-demand periods in the night.

Heat demand was assumed to vary across typical days as depicted in Fig. 16. According to the input data used, there was little impact of RES output levels during spring and autumn on heat demand levels; therefore, the same profiles have been used for both low- and high-RES output day variants.

In order for the case study to be compatible with the energy system decarbonisation agenda, a zero-carbon constraint has been enforced for heat production, which effectively only allowed HP and TES capacity to be built, and prevented investing in gas-fired CHP units or boilers. Investment cost assumptions were the same as in Table 1.

Table 3 presents the summary of optimisation results for the Low and High RES share systems, including the installed capacities, annual heat output and investment and operation cost categories. Note that the difference in total heat demand is due to different typical day frequencies used in the two system scenarios. Nevertheless, the average cost of unit of heat is almost the same for both scenarios (€30.2/MWh_{th}).

Investment decisions for HP capacities are similar in both systems, with about 3% less capacity built in the High RES share system. The optimal capacity of TES in the High RES share scenario, characterised by higher price volatility, is 1.63 MW_{th}, which is about 11% higher than in the Low RES share system (1.47 MW_{th}). Despite the difference in HP capacities, the annual heat output of HP is almost the same in both scenarios (4.73 GWh_{th}), although the annual HP operation cost (i.e. the cost of purchasing electricity) is about 1.5% lower in the High RES share system. Lower operating cost is enabled by higher TES capacity and more volatile electricity prices, allowing HPs to take advantage of periods with very low or even negative prices. Also, lower cost of electricity is achieved despite the average electricity price over the year in both systems being approximately the same, and the prices on winter peak day being evidently higher in the High RES share system (Fig. 15). This emphasises the value of heat storage for managing electricity price volatility in systems with electrified heat production and high RES penetration.

To further illustrate how the optimisation results are driven by the underlying price profiles, variations in operating patterns of HP and TES are presented in Fig. 17 for low- and high-RES output variants of spring days for the two system scenarios. In both scenarios the HP and TES operation changes in response to low or negative prices, so that the use of HP is maximised during the period between 9am and 5 pm, which is markedly different from the low-RES output day with normal prices. Excess heat output from HP during low or negative price periods is stored into TES, to be used at other times of the day (early mornings and evenings).

Although not directly visible from Fig. 17, more heat is stored into TES between about 9am and 5pm in the High RES share scenario than in the Low RES share scenario, justifying the installation of higher TES capacity in the latter case. This is further illustrated in Fig. 18, which shows the variations in heat storage SoC during high-RES output spring day variant for both system scenarios. In the High RES share system scenario the charging of TES during negative price periods starts earlier

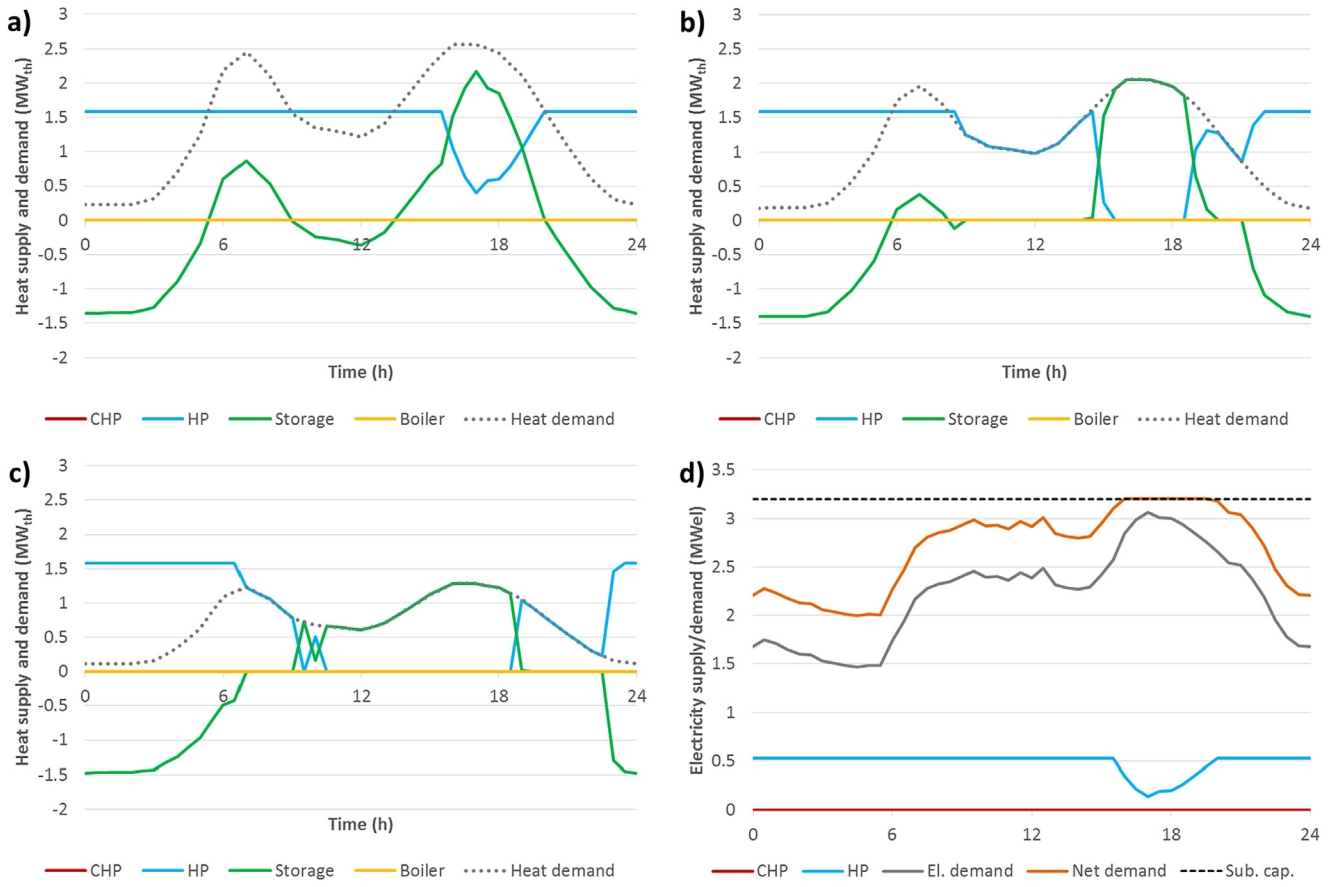

Fig. 14. Heat supply profiles in Case C for: a) winter peak, b) winter average and c) spring/autumn average day; d) total loading of local distribution substation for winter peak day.

and involves a higher volume of heat (6.54 MWh_{th}) than in the Low RES share system (5.86 MWh_{th}) characterised by low but positive prices on high-RES output days. In other words, more volatile prices increase the optimal level of TES capacity.

3.7. Sensitivity of cost-optimal TES capacity to system conditions

This section discusses the results of further sensitivity analysis with the purpose of quantifying the impact of installed TES capacity on the total net cost of heat supply i.e. the objective function formulated in (1). It also investigates in more detail the sensitivity of the cost-optimal volume of TES capacity to assumptions on local grid constraints and the volatility of electricity prices reflecting the share of RES in electricity supply.

To illustrate how variations in installed TES capacity affect the net cost objective function, Fig. 19 shows the unit cost of heat supply as a function of TES capacity for three scenarios:

- Flat price scenario, with a constant electricity price equal to the annual average price of the High RES Share scenario (€42.3/MWh);

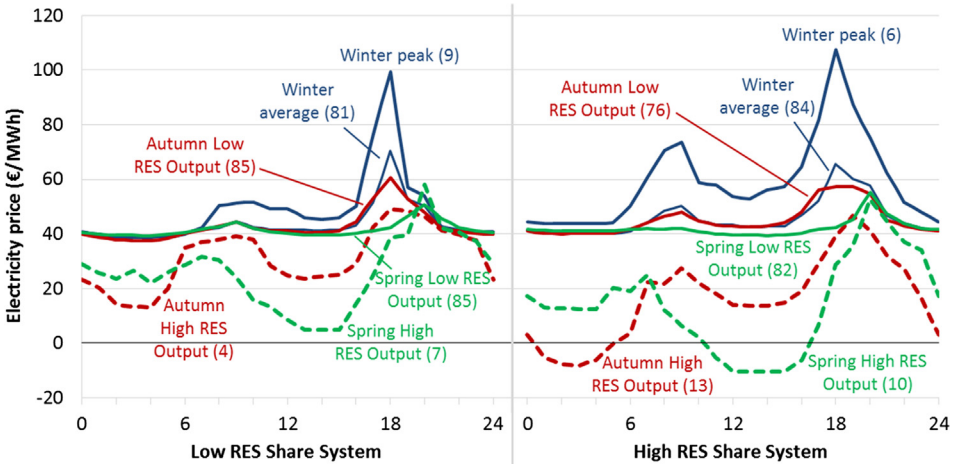

Fig. 15. Electricity price profiles for typical days in Low RES share and High RES share systems (numbers in brackets refer to frequencies of occurrence of typical days).

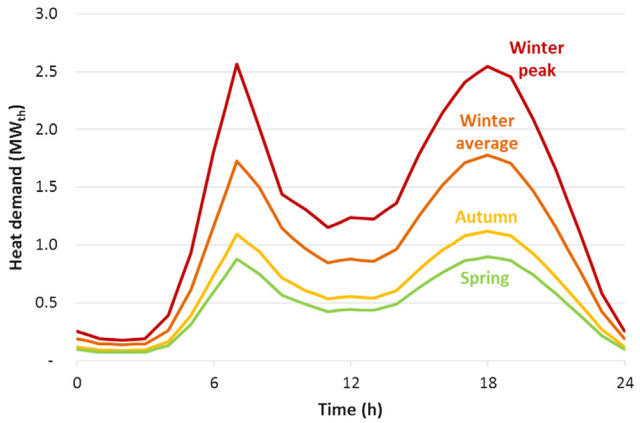

Fig. 16. Heat demand profiles for typical days used in the case study in Section 3.6.

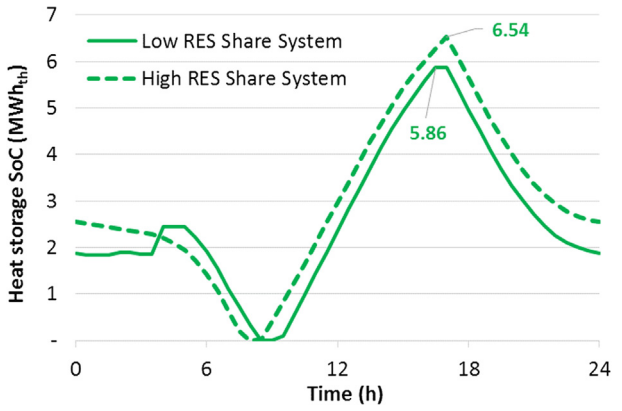

Fig. 18. Heat storage SoC for high-RES output spring day for two system scenarios.

Table 3
Optimisation results for Low and High RES share systems.

Result	*Low RES share*	*High RES share*
HP capacity (MW_{el})	0.485	0.470
TES capacity (MW_{th}/MWh_{th})	1.47/5.86	1.63/6.54
Annual heat demand (MWh_{th})	4580	4551
HP heat output (MWh_{th})	4733	4729
TES roundtrip losses (MWh_{th})	153	178
HP investment cost (€/yr)	58,468	56,971
TES investment cost (€/yr)	15,660	17,342
HP operation cost (€/yr)	64,050	63,113
Total cost (€/yr)	138,178	137,426
Average cost of heat (€/MWh_{th})	30.17	30.20

- High RES Share scenario, as described in Section 3.6;
- High RES Share scenario with a local grid constraint of 3.2 MW_{el}.

The three scenarios have been implemented on the case study with 6 characteristic days and a zero carbon target, as elaborated in Section 3.6. TES capacity in all three scenarios was varied between 0 and 2.5 MW_{th} in 0.05 MW_{th} increments. Each TES capacity value was given as fixed input into the model, which was allowed to optimise all decision variables except the TES capacity. The obtained values for the average cost of heat are shown in Fig. 19.

In each scenario the cost of heat will have a minimum point that corresponds to the cost-optimal volume of heat storage, as indicated in Fig. 19. The optimal TES capacity point will vary between different

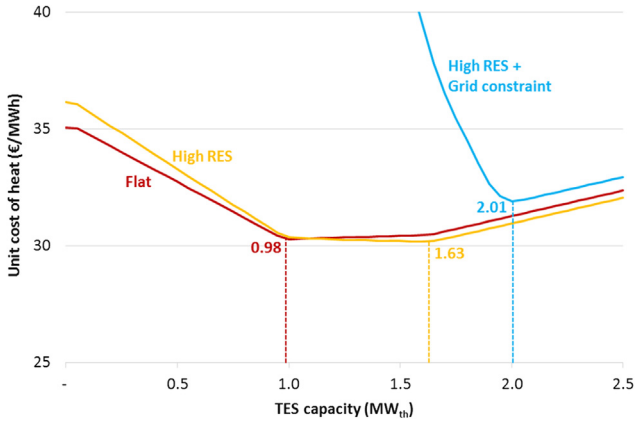

Fig. 19. Impact of TES capacity on the cost of heat supply for Flat price profile and for High RES share price profile with and without local grid constraint.

scenarios, following the fundamental economic principle that TES capacity should be incrementally added to the system up to the point where its marginal benefit (i.e. heat supply cost reduction) becomes lower than the additional cost of installing an incremental unit of storage capacity. Given that the cost per unit capacity of TES was assumed to be the same in all scenarios, different cost-optimal TES capacities indicate that marginal benefits achieved by adding heat storage differ across the three scenarios. Benefits of adding storage are driven by the system cost avoided through adding more storage. The avoided cost in this case consists of lower investment cost of HP capacity, reduced cost

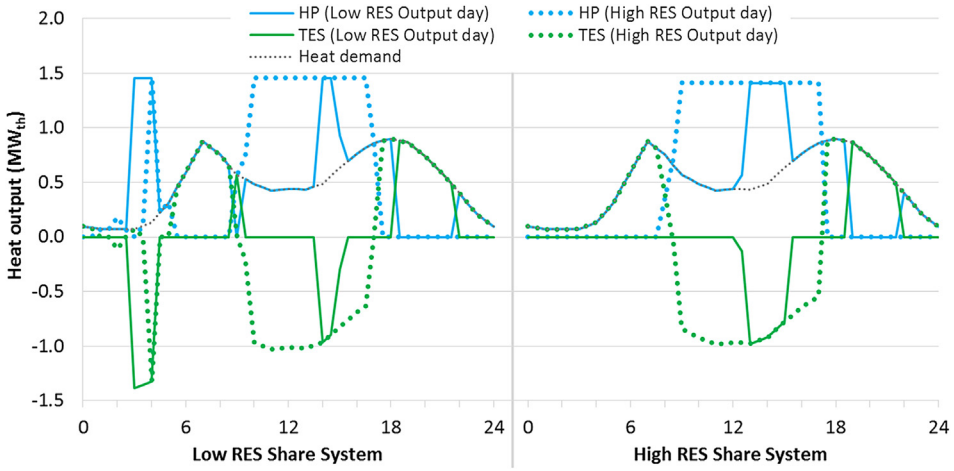

Fig. 17. Heat production profiles for low- and high-RES output spring days for two system scenarios.

of electricity purchases and (where applicable) avoided demand curtailment cost. In the Flat price scenario, the marginal benefit of TES drops to the level of TES investment cost already at around 1 MW_{th}. With more volatile electricity prices characteristic for the High RES Share scenario, more TES capacity (1.6 MW_{th}) can be installed cost-efficiently to take advantage of price arbitrage opportunities including periods of negative prices. Finally, when volatile prices are combined with a local grid constraint, the cost-optimal TES capacity increases to over 2 MW_{th}, given that for any TES capacity lower than that the alternative solution would be either demand curtailment or grid reinforcement (given that HP output is constrained), both of which are very costly.

As already demonstrated, the share of RES in electricity supply reflected in the price volatility and the severity of local grid constraints can significantly increase the cost-optimal volume of TES in the local DH system. To quantify this relationship in more detail, Fig. 20 demonstrates how the optimal TES capacity changes for different levels of local grid constraints, across two electricity price scenarios: (i) High RES Share (same as in Section 3.6), and (ii) Flat (with the constant electricity price same as the average price of the High RES Share scenario). Note that the assumed underlying electricity demand (i.e. before adding any demand by centralised HPs) is given in Fig. 4.

Substation capacity values in this analysis have been varied between 3.1 MW_{el} and 3.8 MW_{el}. If the local substation capacity is constrained to 3.6 MW_{el} or more, there is no impact on the cost-optimal TES capacity in either scenario, as the HP can operate without being constrained by the local grid. The resulting optimal TES volumes are 1.63 MW_{th} and 0.98 MW_{th} for High RES Share and Flat scenarios, respectively. At the lower end of the range, any substation capacity below 3.1 MW_{el} would not be sufficient to meet even the baseline local electricity demand regardless of the heat supply solution, and is therefore not relevant for the analysis.

For grid capacity constraints between 3.1 MW_{el} and 3.45 MW_{el}, the cost-optimal TES capacity is actually the same for both Flat and High RES Share scenarios, suggesting that adding TES in those cases is primarily driven by avoiding high demand curtailment cost, which applies equally in both scenarios. Nevertheless, for grid constraints in the range between 3.45 MW_{el} and 3.55 MW_{el} the cost-optimal TES volumes in the two scenarios diverge significantly given that the benefit of TES becomes increasingly driven by electricity price arbitrage opportunities, which are much more attractive in the High RES Share scenario that is characterised by high price volatility and even negative prices. From around 3.55 MW_{el} the optimal TES capacities for both scenarios converge to the optimal solutions of non-constrained cases.

For the most severe constrained case of 3.1 MW_{el} it can be observed that the cost-optimal TES capacity reaches 2.31 MW_{th} in both scenarios, which is 41% and 134% higher than the optimal capacity in non-constrained cases for High RES Share and Flat scenarios, respectively.

The share of RES in electricity supply and the resulting volatility of electricity prices also represents a key driver for the cost-efficient volume of heat storage. Combining the results for TES capacity obtained for High and Low RES Share scenarios in Table 3 and the result for a Flat price scenario in Fig. 19 (which had the same annual average electricity price), it is evident that price volatility driven by RES share represents a key factor for the higher requirement for TES capacity. The cost-optimal TES capacity increases from 0.98 MW_{th} in the Flat scenario to 1.47 MW_{th} (50% more) in the Low RES Share scenario, and to 1.63 MW_{th} (66% more) in the High RES Share scenario.

4. Conclusions

This paper proposes a novel optimisation approach for modelling local and system-wide interactions between heat and electricity networks addressing planning and operational domains. Decarbonisation of electricity and heat supply presents numerous challenges, but also opportunities for stronger system integration between the two sectors, taking advantage of flexibility in the heat sector to facilitate a higher penetration of intermittent renewable energy and thus a cost-effective decarbonisation of the electricity sector. The modelling approach shows that certain flexible options in the heating system (such as CHPs or TES) could have significant whole-system value that is reflected outside of the local district heating application. As shown in the case studies and the associated sensitivity analysis, it may be beneficial to increase the size of TES or CHP beyond the locally optimised solution, in order to provide additional flexibility in the interactions with the electricity grid and help with managing local network constraints or local emission targets. For instance, an increase in cost-optimal TES capacity of 41–134% has been observed in cases where the local heating system also had to consider a severe constraint in the local electricity distribution grid. At the same time, higher RES penetration scenarios reflected in higher electricity price volatility have also been shown to increase the optimal size of local thermal storage by 50–66% compared to a constant price scenario, allowing centralised electric HP technologies to divert excess electricity produced by intermittent renewable generators to the heating sector. It is therefore crucial to reflect the whole-system value of flexible heating technologies in the underlying cost-benefit analysis of heat networks, especially in the context of overall energy system decarbonisation.

Future work on extending the functionality of the model will focus on: adding cooling demand and supply, increasing the detail on technologies representation and the size range of options, reformulating the objective function from minimisation of annualised cost to maximisation of profit, further refining the operating parameters of CHP and HP plants where appropriate (e.g. by considering ramping constraints, variable H/E ratios and seasonal COP variations, limited number of starts per day, etc.), and including the provision of ancillary services (e.g. frequency regulation) as a potential additional source of revenue for CHP and HP assets. Another important area that will be explored is the integration of heat generation technologies planning and heat network design (such as the one presented in [37] or [57]) to enable co-optimisation of both heat network and generation assets while considering the interactions with the electricity system.

CRediT authorship contribution statement

Marko Aunedi: Conceptualization, Methodology, Software, Writing - original draft. **Antonio Marco Pantaleo:** Writing - review & editing, Investigation. **Kamal Kuriyan:** Writing - review & editing, Validation. **Goran Strbac:** Conceptualization, Resources. **Nilay Shah:** Funding acquisition, Supervision.

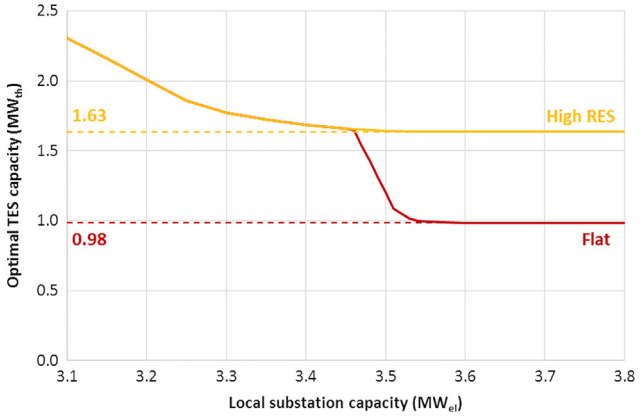

Fig. 20. Variation in optimal TES capacity as function of local substation capacity for Flat and High RES Share price profiles.

Declaration of Competing Interest

The authors declare that they have no known competing financial interests or personal relationships that could have appeared to influence the work reported in this paper.

Acknowledgment

The research presented in this paper has been supported by European Union's Horizon 2020 research and innovation programme under grant agreement No. 723636 (THERMOS), and by the UK Engineering and Physical Sciences Research Council (EPSRC) grant numbers EP/R045518/1 and EP/S031898/1. The authors also acknowledge the support and feedback obtained from the Centre for Sustainable Energy (www.cse.org.uk) in their role as THERMOS project leader, and in particular the contributions from Joshua Thumim, Tom Hinton and Martin Holley.

References

[1] Communication from the Commission to the European Parliament, the Council, the European Economic and Social Committee and the Committee of the Regions: An EU Strategy on Heating and Cooling, COM; 2016. p. 51. https://ec.europa.eu/energy/sites/ener/files/documents/1_EN_ACT_part1_v14.pdf [accessed 24 January 2020].
[2] Zhang X, Strbac G, Teng F, Djapic P. Economic assessment of alternative heat decarbonisation strategies through coordinated operation with electricity system – UK case study. Appl Energy 2018;222:79–91.
[3] Imperial College London, Analysis of alternative UK heat decarbonisation pathways (report for the CCC); 2018. https://www.theccc.org.uk/publication/analysis-of-alternative-uk-heat-decarbonisation-pathways/ [accessed 24 January 2020].
[4] Lund H, Möller B, Mathiesen BV, Dyrelund A. The role of district heating in future renewable energy systems. Energy 2010;35:1381–90.
[5] Lund H, Werner S, Wiltshire R, Svendsen S, Thorsen JE, Hvelplund F, et al. Generation District Heating (4GDH): Integrating smart thermal grids into future sustainable energy systems. Energy 2014;68:1–11.
[6] Gabrielli P, Gazzani M, Martelli E, Mazzotti M. Optimal design of multi-energy systems with seasonal storage. Appl Energy 2018;219:408–24.
[7] Erdener BC, Pambour KA, Lavin RB, Dengiz B. An integrated simulation model for analysing electricity and gas systems. Int J Electr Power Energy Syst 2014;61:410–20.
[8] Bai L, Li F, Cui H, Jiang T, Sun H, Zhu J. Interval optimization based operating strategy for gas-electricity integrated energy systems considering demand response and wind uncertainty. Appl Energy 2016;167:270–9.
[9] Cui H, Li F, Hu Q, Bai L, Fang X. Day-ahead coordinated operation of utility-scale electricity and natural gas networks considering demand response based virtual power plants. Appl Energy 2016;176:183–95.
[10] Li G, Zhang R, Jiang T, Chen H, Bai L, Li X. Security-constrained bi-level economic dispatch model for integrated natural gas and electricity systems considering wind power and power-to-gas process. Appl Energy 2017;194:696–704.
[11] Zeng Q, Zhang B, Fang J, Chen Z. A bi-level programming for multistage co-expansion planning of the integrated gas and electricity system. Appl Energy 2017;200:192–203.
[12] Alabdulwahab A, Abusorrah A, Zhang X, Shahidehpour M. Coordination of interdependent natural gas and electricity infrastructures for firming the variability of wind energy in stochastic day-ahead scheduling. IEEE Trans Sustainable Energy 2015;6:606–15.
[13] Kirkerud JG, Trømborg E, Bolkesjø TF. Impacts of electricity grid tariffs on flexible use of electricity to heat generation. Energy 2016;115:1679–87.
[14] Balić D, Lončar D. Impact of fluctuating energy prices on the operation strategy of a trigeneration system. J Sustain Develop Energy Water Environ Syst 2015;3:315–32.
[15] Pantaleo AM, Camporeale S, Shah N. Natural gas-biomass dual fuelled micro-turbines: Comparison of operating strategies in the Italian residential sector. Appl Therm Eng 2014;71:686–96.
[16] Camporeale SM, Ciliberti PD, Fortunato B, Torresi M, Pantaleo AM. Externally fired micro-gas turbine and organic rankine cycle bottoming cycle: optimal biomass/natural gas combined heat and power generation configuration for residential energy demand. J Eng Gas Turbines Power 2016;139.
[17] Pantaleo AM, Camporeale SM, Sorrentino A, Miliozzi A, Shah N, Markides CN. Hybrid solar-biomass combined Brayton/organic Rankine-cycle plants integrated with thermal storage: Techno-economic feasibility in selected Mediterranean areas. Renewable Energy 2020;147:2913–31. https://doi.org/10.1016/j.renene.2018.08.022.
[18] Pantaleo AM, Camporeale SM, Miliozzi A, Russo V, Shah N, Markides CN. Novel hybrid CSP-biomass CHP for flexible generation: Thermo-economic analysis and profitability assessment. Appl Energy 2017;204:994–1006.
[19] Rubio-Maya C, Uche-Marcuello J, Martínez-Gracia A, Bayod-Rújula AA. Design optimization of a polygeneration plant fuelled by natural gas and renewable energy sources. Appl Energy 2011;88:449–57.
[20] Department of Energy & Climate Change, Heat Pumps in District Heating; 2016, https://www.gov.uk/government/publications/heat-pumps-in-district-heating [accessed 24 January 2020].
[21] Østergaard PA, Andersen AN. Booster heat pumps and central heat pumps in district heating. Appl Energy 2016;184:1374–88.
[22] Blarke MB, Lund H. Large-scale heat pumps in sustainable energy systems: system and project perspectives. Therm Sci 2007;11:143–52.
[23] Hast A, Rinne S, Syri S, Kiviluoma J. The role of heat storages in facilitating the adaptation of district heating systems to large amount of variable renewable electricity. Energy 2017;137:775–88.
[24] Abdollahi E, Lahdelma R. Decomposition method for optimizing long-term multi-area energy production with heat and power storages. Appl Energy 2020;260.
[25] Connolly D, Lund H, Mathiesen BV, Werner S, Möller B, Persson U, et al. Heat Roadmap Europe: Combining district heating with heat savings to decarbonise the EU energy system. Energy Policy 2014;65:475–89.
[26] Werner S. International review of district heating and cooling. Energy 2017;137:617–31.
[27] Rezaie B, Rosen MA. District heating and cooling: Review of technology and potential enhancements. Appl Energy 2012;93:2–10.
[28] Nielsen S. A geographic method for high resolution spatial heat planning. Energy 2014;67:351–62.
[29] Karlsson KB, Petrović SN, Næraa R. Heat supply planning for the ecological housing community Munksøgård. Energy 2016;115:1733–47.
[30] Weber C, Shah N. Optimisation based design of a district energy system for an eco-town in the United Kingdom. Energy 2011;36:1292–308.
[31] Li H, Svendsen S. District Heating network design and configuration optimization with genetic algorithm. J Sustain Develop Energy Water Environ Syst 2013;1:291–303.
[32] Fang T, Lahdelma R. Genetic optimization of multi-plant heat production in district heating networks. Appl Energy 2015;159:610–9.
[33] Jing Rui, Wang Meng, Zhang Zhihui, Wang Xiaonan, Li Ning, Shah Nilay, Zhao Yingru. Distributed or centralized? Designing district-level urban energy systems by a hierarchical approach considering demand uncertainties. Appl Energy 2019;252:113424. https://doi.org/10.1016/j.apenergy.2019.113424.
[34] Lambert RSC, Maier S, Shah N, Polak JW. Optimal phasing of district heating network investments using multi-stage stochastic programming. Int J Sustain Energy Plan Manage 2016;9:57–74.
[35] Jing R, Wang M, Liang H, Wang X, Li N, Shah N, et al. Multi-objective optimization of a neighborhood-level urban energy network: Considering Game-theory inspired multi-benefit allocation constraints. Appl Energy 2018;231:534–48.
[36] Bordin C, Gordini A, Vigo D. An optimization approach for district heating strategic network design. Eur J Oper Res 2016;252:296–307.
[37] Kuriyan K, Shah N. A combined spatial and technological model for the planning of district energy systems. Int J Sustain Energy Plan Manage 2019;21:111–31.
[38] Unternährer J, Moret S, Joost S, Maréchal F. Spatial clustering for district heating integration in urban energy systems: Application to geothermal energy. Appl Energy 2017;190:749–63.
[39] Wang H, Duanmu L, Lahdelma R, Li X. Developing a multicriteria decision support framework for CHP based combined district heating systems. Appl Energy 2017;205:345–68.
[40] Delangle A, Lambert RSC, Shah N, Acha S, Markides CN. Modelling and optimising the marginal expansion of an existing district heating network. Energy 2017;140:209–23.
[41] Pieper H, Masatin V, Volkova A, Ommen T, Elmegaard B, Markussen WB. Modelling framework for integration of large-scale heat pumps in district heating using low-temperature heat sources: A case study of Talinn, Estonia. Int J Sustain Energy Plan Manage 2019;20:67–86.
[42] Murray P, Orehounig K, Grosspietsch D, Carmeliet J. A comparison of storage systems in neighbourhood decentralized energy system applications from 2015 to 2050. Appl Energy 2018;231:1285–306.
[43] Fang T, Lahdelma R. Evaluation of a multiple linear regression model and SARIMA model in forecasting heat demand for district heating system. Appl Energy 2016;179:544–52.
[44] Acha S, Bustos-Turu G, Shah N. Modelling real-time pricing of electricity for energy conservation measures in the UK commercial sector. 2016 IEEE international energy conference (ENERGYCON). 2016.
[45] Li Z, Wu W, Wang J, Zhang B, Zheng T. Transmission-constrained unit commitment considering combined electricity and district heating networks. IEEE Trans Sustainable Energy 2016;7:480–92.
[46] Najafi A, Falaghi H, Contreras J, Ramezani M. Medium-term energy hub management subject to electricity price and wind uncertainty. Appl Energy 2016;168:418–33.
[47] Nazari-Heris M, Mohammadi-Ivatloo B, Gharehpetian GB, Shahidehpour M. Robust short-term scheduling of integrated heat and power microgrids. IEEE Syst J 2018;99:1–9.
[48] Ali Shaabani Y, Seifi AR, Kouhanjani MJ. Stochastic multi-objective optimization of combined heat and power economic/emission dispatch. Energy 2017;141:1892–904.
[49] Lu S, Gu W, Zhou J, Zhang X, Wu C. Coordinated dispatch of multi-energy system with district heating network: Modeling and solution strategy. Energy 2018;152:358–70.
[50] Alipour M, Mohammadi-Ivatloo B, Zare K. Stochastic scheduling of renewable and CHP-based microgrids. IEEE Trans Ind Inf 2015;11:1049–58.
[51] Jiménez Navarro JP, Kavvadias KC, Quoilin S, Zucker A. The joint effect of centralised cogeneration plants and thermal storage on the efficiency and cost of the power system. Energy 2018;149:535–49.

[52] Zhang X, Strbac G, Shah N, Teng F, Pudjianto D. Whole-System Assessment of the Benefits of Integrated Electricity and Heat System. IEEE Trans Smart Grid 2019;10:1132–45.
[53] THERMOS (Thermal Energy Resource Modelling and Optimisation System) project, https://www.thermos-project.eu/home/ [accessed 24 January 2020].
[54] Falke T, Krengel S, Meinerzhagen A-K, Schnettler A. Multi-objective optimization and simulation model for the design of distributed energy systems. Appl Energy 2016;184:1508–16.
[55] Dorotić H, Pukšec T, Duić N. Multi-objective optimization of district heating and cooling systems for a one-year time horizon. Energy 2019;169:319–28.
[56] Jiménez Navarro JP, Cejudo López JM, Connolly D. The effect of feed-in-tariff supporting schemes on the viability of a district heating and cooling production system. Energy 2017;134:438–48.
[57] Pantaleo AM, Giarola S, Bauen A, Shah N. Integration of biomass into urban energy systems for heat and power Part I: An MILP based spatial optimization methodology. Energy Convers Manage 2014;83:347–61.
[58] U.S. Environmental Protection Agency, Catalog of CHP Technologies: Section 2. Technology Characterization – Reciprocating Internal Combustion Engines, March 2015. https://www.epa.gov/chp/catalog-chp-technologies [accessed 28 January 2020].
[59] FICO® Xpress Optimization, https://www.fico.com/en/products/fico-xpress-optimization [accessed 24 January 2020].
[60] Capuder T, Mancarella P. Techno-economic and environmental modelling and optimization of flexible distributed multi-generation options. Energy 2014;71:516–33.
[61] Bhatia SC. Cogeneration. Advanced renewable energy systems. Woodhead Publishing India; 2014. p. 490–508.
[62] Pudjianto D, Aunedi M, Djapic P, Strbac G. Whole-system assessment of value of energy storage in low-carbon electricity systems. IEEE Trans Smart Grid 2014;5:1098–109.